

**Assessment of Classification Methods
based on Structure from Motion Point Clouds
for monitoring dynamic River Environments**

by

Jakob Iglhaut

Master's Thesis

Submitted in partial fulfillment of the requirements of the degree

Master of Science in Engineering

Spatial Information Management

Carinthia University of Applied Sciences

School of Engineering & IT

Department of Geformation & Environmental Technologies

External Supervisors:

Prof. Dr. İnci Güneralp, Department of Geography, Texas A&M University, Texas,
United States of America

Prof. Dr. Anthony Filippi, Department of Geography, Texas A&M University, Texas,
United States of America

Internal Supervisors:

FH-Prof. Mag. Dr. Gernot Paulus MSc. MAS, School of Spatial Information
Management, Carinthia University of Applied Sciences, Villach, Austria

FH-Prof. Dr.-Ing. Karl-Heinrich Anders, School of Spatial Information Management,
Carinthia University of Applied Sciences, Villach, Austria

Villach, 07.09.2016

Acknowledgements

I take this opportunity to express my gratitude to the people who have been instrumental in the successful completion of this thesis. Prof. Dr. Filippi and Prof. Dr. Güneralp, of the Department of Geography at Texas A&M University who I had the honor to collaborate with during my four months stay in College Station. They provided me with a very welcoming atmosphere and I am deeply thankful for their input on fluvial sciences. Of course this research exchange would not have been possible without the financial support of the Marshall Plan Foundation. I want to thank the foundation for giving me this great opportunity. I also want show my appreciation to my supervisors at the Carinthia University of Applied Sciences, FH-Prof. Mag. Dr. Gernot Paulus and FH-Prof. Dr.-Ing. Karl-Heinrich Anders for letting me use this topic and for their guidance during the project. Lastly I would like to acknowledge Martin Isenburg, founder of rapidlasso GmbH, who generously provided me with a full license to his brilliant software LAsTools which generally enabled most of the performed processing tasks.

Thank you!

Statutory Declaration

I hereby declare that:

- the Master thesis has been written by myself without any external unauthorized help and that it has not been submitted to any institution to achieve an academic grading.
- I have not used sources or means without citing them in the text; any thoughts from others or literal quotations are clearly marked.
- the electronically submitted Master thesis is identical to the hard copy.
- one copy of the Master thesis is deposited and made available in the CUAS library (§ 8 Austrian Copyright Law [UrhG]).

Place, Date

Signature

Abstract

Surveying methods for monitoring rivers traditionally rely on tedious field work. Such point or line sampling however does not fully illustrate these dynamic environments in their temporal and spatial heterogeneity. Data representing the “riverscape” at high resolution is in increasing demand to assess geomorphic dynamics, flow hydraulics, in-stream habitat and other process-oriented investigations. Parallel advancements in light-weight, small-scale unmanned aerial systems (UAS) and photogrammetry using Structure from Motion (SfM) algorithms have resulted in an explosion of uses for inexpensive and easily obtained remotely sensed data. Here point clouds, the primary output of a SfM approach, are evaluated for their potential to provide data towards holistic monitoring of rivers. Point clouds utilized in this study stem from the Remotely Piloted Aircraft multi Sensor System (RPAmSS), a small-scale UAS equipped with a consumer grade camera for 2D and 3D mapping. For two different river systems, both subject to the EU-LIFE restoration project, multispectral imagery was acquired at hyperspatial resolutions ($<0.1\text{m}$) and point clouds were photogrammetrically derived. First, the point clouds were referenced to address observed shifts in their absolute location. Further preprocessing steps include subsampling and noise filtering. Five classification and ground filtering methods were applied and assessed for their performance on SfM point clouds. Results show that the proprietary software LAStools offered the overall best functionality. The open-source Cloth Simulation Filter was identified as fast and reliable bare-earth extraction tool. Further results are the workflow for the calculation of ratio based indices on point clouds using merged RGB and NIR data. Finally the submerged bathymetry was estimated considering the refraction of water. Compared to sonar cross sections underwater topography was derived at $\text{RMSE} = 0.33\text{m}$ before and $\text{RMSE} = 0.19\text{m}$ after refraction correction.

Keywords:

structure from motion; unmanned aerial system, photogrammetry; river; monitoring; fluvial; bathymetry; point cloud; classification; filtering

Table of Contents

1	Introduction.....	5
1.1	Motivation	5
1.2	Goals and Problem Definition	7
1.3	Expected Results.....	9
1.4	Thesis Overview	9
2	State-of-the-Art	10
2.1	River Vegetation	10
2.2	Geomorphology of Rivers.....	10
2.3	Unmanned Aerial Systems / RPAmSS.....	11
2.4	Point Clouds.....	12
2.5	Point Cloud Acquisition Approaches	13
2.5.1	LiDAR	13
2.5.2	Photogrammetry	14
2.6	Point Cloud Classification	18
2.7	Ratio-based Spectral Indices	21
2.8	Fluvial Topography	22
2.9	Comparison of Point Clouds.....	24
3	Methods	25
3.1	Study areas	25
3.2	Geodata Sources.....	27
3.3	Concept.....	29
3.4	Preprocessing	30
3.5	Classification	32
3.6	Spectrally Derived Indices on Point Clouds.....	35
3.7	Bathymetry Estimation.....	36

4	Implementation	37
4.1	Preprocessing	38
4.1.1	Projection	38
4.1.2	Sub-sampling	38
4.1.3	Referencing.....	40
4.1.4	Noise Filtering.....	43
4.2	Classification	45
4.3	Spectrally Derived Indices on Point Clouds.....	49
4.4	Bathymetry Estimation	50
4.4.1	Water Boundary Extraction	50
4.4.2	Refraction Correction	52
5	Results	54
5.1	Classification	54
5.2	NDVI and NDWI Point Cloud.....	58
5.3	Quantified Submerged Topography.....	59
6	Discussion	63
7	Future Work.....	66
8	References.....	69
	Annex	74

List of Abbreviations

AGL	Above Ground Level
ASL	Above Sea Level
C2C	Cloud-to-Cloud
C2M	Cloud-to-Mesh
DEM	Digital Elevation Model
DoD	DEM of Difference
DSM	Digital Surface Model
DTM	Digital Terrain Model
GSD	Ground Sampling Distance
IMU	Inertia Measurement Unit
LiDAR	Light Detection And Ranging
MVS	Multi-View Stereo
RMSD	Root Mean Square Deviation
RPAmSS	Remotely Piloted Aircraft multi Sensor System
RTK	Real Time Kinematic
SfM	Structure from Motion
TLS	Terrestrial Laser Scanning / Scanner
UAS	Unmanned Arial System
UAV	Unmanned Arial Vehicle

1 Introduction

1.1 Motivation

Traditionally river ecosystem management relies on tedious field sampling methods for monitoring purposes. Such approach inevitably forces river scientists to look at these ecosystems with a narrow field of view that doesn't illustrate the three-dimensionality and dynamics of these complex systems (Carbonneau and Piégay 2012). The modern fluvial geomorphology and ecology domain recognizes that natural processes of biotic and abiotic nature are to be seen as part of a holistic river system, which can only be represented by non-localized and continuous data capture (Fausch *et al.* 2002, Wiens 2002, Carbonneau and Piégay 2012, Dietrich 2016). A flexible multidisciplinary approach operating at broad spatial and temporal scales is hence needed to perform monitoring that is truly representative to the matter. Only remote sensing techniques hold the potential to objectively capture river environments in such a way. Solely spatially inclusive and comprehensive data facilitates a better understanding of their dynamics.

Fluvial landscapes are unique in a way that in order to study these environments they require a blend of multiple disciplines: hydrology, ecology and geomorphology (Pool 2002). Logically the remotely sensed data needs to reflect the information valuable for these fields of study. An arrangement of sensors is needed to obtain data on the heterogenic characteristics of the lotic ecosystem at high-resolution. The recent advances in remote sensing technologies, especially in the unmanned aerial system (UAS) sector, allow for the desired time and cost efficient data collection, facilitating broad scale surveys at frequent time scales (Javernick *et al.* 2014). The ongoing research and development project RPAmSS at Carinthia University of Applied Sciences evaluates the potential of a “Remotely Piloted Aircraft multi Sensor System” for the fast and high-resolution capture of multidimensional environmental data. With two test sites in scope flights are carried out at the rivers Gail and Drau, near Villach, Austria. Both test sites are subject to the LIFE-Project, a river revitalization program within the framework of the EU LIFE-Nature conservation. Within the LIFE-Project valuable habitats for flora and fauna are better protected and flood protection is being improved. As a progressive approach to capture data to monitor these environments the fixed-wing RPAmSS is currently equipped with an APS-C size sensor camera offering high-resolution multispectral imagery. RGB and NIR imagery has been acquired throughout different seasons since the start of the project. The low altitude flights enable capturing imagery with very small ground sampling distance (GSD), making for a well suited basis for studying the complex environments present on these sites (Zander 2015). Not only can this imagery be used for common raster based analyses but dense point clouds representing the terrain and features may be derived photogrammetrically. Although light detection and ranging (LiDAR) based systems are nowadays commonly used for topographic analyses of the environment they are laborious and costly to implement for river assessments. For terrestrial laser scans the sensor has to be set up at numerous points throughout the river system, in order to capture entire fluvial landscapes, making it a labor-intensive procedure (Smith and Vericat 2014). Airborne LiDAR on the other hand is expensive because of the numerous turns the plane has to perform to achieve straight parallel survey lines over the area of interest. This is due to the curvilinear nature of rivers (Pool 2002). To acquire information within the submerged part of the channel so called bathymetric LiDAR systems are required (Kinzel *et al.* 2013). Fully quantifying topography of river environments by LiDAR depends on two separate systems with different wavelengths dry and water covered areas. Here a photogrammetric approach for point cloud creation, based on a flexibly

deployed UAS, can potentially deliver information of dry bed topography and submerged bathymetry with one technology (Woodget *et al.* 2015). Although the combined use of UAS and so called Structure from Motion photogrammetry offers relatively inexpensive acquisition three dimensional data such approach has seen little evaluation for applications in riverine science and management (Fonstad *et al.* 2013b). Yet, with the objective to monitor river systems holistically, point cloud data holds certain advantages over two-dimensional data. Analyzing point clouds aims directly at gaining insights in the three dimensional structures of river environments (Pool 2002, Fonstad *et al.* 2013a). Point cloud methods help to preserve the accuracy of the original data while comprising of more information in regard to topographic change, than a typical raster analysis. Relevant not only to geomorphological features of the fluvial system point clouds can also facilitate studies on the riparian vegetation in steep features of river banks (Brasington *et al.* 2012, Brodu and Lague 2012, Lague 2014). However investigations on the heterogeneous surfaces of vegetation and ground require separation into relevant classes. Distinguishing between the diverse morphological properties of features in fluvial environments yields a wide range of applications in the field of river sciences and management including geomorphic change detection (Legleiter 2014b, 2014a) analyses on dune fields and vegetation hydraulic roughness (Barnea *et al.* 2007), channel bed dynamics (Milan *et al.* 2007), cliff erosion and rockfall characteristics (Rosser *et al.* 2005, Abellán *et al.* 2006) and grain size distribution (Hodge *et al.* 2009a, 2009b).

1.2 Goals and Problem Definition

The main goal of the current study lies in the evaluation of using photogrammetric point cloud data in for river monitoring applications. Central to this study is the classification and bare-earth extraction of Structure from Motion point clouds. Further areas of application addressed here are the calculation of spectrally derived indices and the quantification of submerged bathymetry.

It will be examined whether photogrammetric point clouds, obtained from the RPAmSS, offer sufficient geometrical and positional accuracy towards remotely sensed fluvial studies. Necessary preprocessing steps will be determined and the collected data will be assessed for its' representation of the channel.

Furthermore the study evaluates how well various available classification and ground filtering algorithms can differentiate riverine features based on their geometric properties. Hereby

indices derived from the identified ground surface, such as soil surface roughness, are the basis for erosion models and other applications crucial to river management (Marzahn *et al.* 2010, Grims *et al.* 2014). Current classification approaches are primarily designed for LiDAR data. However it is known that photogrammetric approaches based on low-altitude platforms can produce point clouds with point densities comparable or higher than airborne LiDAR, with horizontal and vertical precision in the centimeter range (Fonstad *et al.* 2013b). Although a more detailed representation of a scene is achievable with a SfM approach the passive acquisition method does not allow for penetration of vegetation resulting in different geometrical properties compared LiDAR point clouds. With these differences in mind the algorithms will be tested for their performance on SfM point clouds representing river scenes.

The RPAmSS acquired point cloud data depicts of spectral information in RGB and NIR. Exploiting this information to derive ratio based indices, such as the common Normalized Difference Vegetation Index, can be an important reference for fluvial scientist. Currently for spectrally based analyses predominantly raster data are utilized. As part of this study a method to create multispectral point clouds will be established to assess the benefit of three dimensional vegetation and water indices for river monitoring.

Topography is the most basic descriptor of geomorphology and holds potential for a range of applications such as geomorphic change detection (Legleiter 2014a, 2014b), analyses channel bed dynamics (Milan *et al.* 2007) and the prediction of velocity conditions which are critical to riverine habitats (Carbonneau and Piégay 2012). Of specific interest to fluvial science is the submerged part of the channel. The remotely sensed estimation of submerged bathymetry however still heavily relies spectral depth approaches based on raster data (Carbonneau and Piégay 2012). Currently there is only one published example of using a UAS-SfM method for the quantification of submerged topography (Woodget *et al.* 2015). A SfM approach however holds the advantage over spectral depth or bathymetric LiDAR acquisition of channel bed information that it can be used as a singular technique for dry and wet topography. While previous work solely used 2D grid data the current study seeks to utilize point clouds for the quantification of submerged bathymetry.

1.3 Expected Results

The major aim of the study lies in evaluating the potential of photogrammetric point clouds for spatially inclusive monitoring of river environments. The following intermediate results are expected:

- Pre-processed multi-temporal point cloud datasets containing multispectral information
- Classified point clouds taking geometry in consideration as well as an objective comparison of results by the different methods used
- A method for the derivation of ratio based indices from multispectral point clouds
- A workflow to quantify submerged topography with SfM point clouds and spatial comparison of results to sonar reference
- Validation of results concerning the achieved accuracy and precision, taking expert knowledge into account

1.4 Thesis Overview

The thesis is organized as follows: In the “State-of-the-Art” chapter previous work is reviewed and analyzed. The background for remotely sensing river environments is given with special focus on the fluvial vegetation and geomorphology. Furthermore a technical overview is given for unmanned aerial systems and the specifics of the platform used for data capture in the current study. The basis of gathering and working with point cloud data is explained with particular focus on Structure from Motion photogrammetry. Furthermore a thorough review of up to date point cloud classification and ground filtering methods is given. The background for the calculation of spectral indices is introduced and the quantification of fluvial topography is outlined in its theory. The chapter “Comparison of point clouds” lays the basis of validation techniques applied to results which forms the knowledge base needed in order to draw meaningful conclusions towards the potential of point clouds remotely monitoring river ecosystems. The conceptual model to carry out the study is presented in the “Methods”. The study area and the data acquisition approach is described to get a full understanding of the basic conditions. All main steps that are undertaken, point cloud pre-processing, classification, calculation of spectral indices and estimation of underwater topography are elaborated on in detail. Respective results are presented in the “Results” chapter and are subsequently

discussed based on qualitative assessment and expert opinion. Conclusions are drawn and ideas on future work on point cloud analyses of natural environments are indicated.

2 State-of-the-Art

2.1 River Vegetation

The characteristics and distribution of riparian vegetation and plant communities in the vicinity of rivers are defined by climate, topography, water availability and the chemical and physical properties of the soil. Not only does the quantity and properties of the vegetation give insight in the ecosystem function but they can directly affect stream channel characteristics (Wang *et al.* 2014). Erosion processes are moderated by root systems in the river banks as they are able to bind deposited sediment. Woody debris on the other hand can initiate bank erosion as well as sediment deposition by deflecting the stream flow (Gippel 1995). Freshly generated bare earth surface, induced either by such process can be repopulated by well adapted pioneer species which at later successional stages are replaced by species that can grow in more shaded and protected conditions. These dynamic changes in plant communities have to be recognized when observing fluvial systems with a holistic view. Knowledge about the abundant river vegetation also presents key information for hydrodynamic modelling as used for analyzing flood hazards. It is of particular importance to understand the hydraulic resistance of fluvial vegetation in order to draw conclusions of how the flow is affected by the surface roughness of the flora (Darby 1999).

2.2 Geomorphology of Rivers

The morphology of fluvial systems is subject to many factors. Generally rivers are influenced by the discharge and slope of the stream as well as the sediment load and the respective sediment size (Wang *et al.* 2014). It is known that rivers adjust their profile and pattern to minimize stream power as present in flowing water to ideally reach equilibrium where the influencing factors are balanced (Lane 1954). However due to changes in seasonal flow and other manipulating biotic and abiotic factors true equilibrium is never reached. Lane 1954 states that “fluvial morphology is therefore the science of the form as produced by the action of flowing water”. The geomorphology of natural dynamic riverine systems is hence a constantly changing environment.

Analyzing the characteristics of the fluvial geomorphology in terms of grain size distribution, sediment deposition and eroded surface is thus crucial to gain better understanding of the river characteristics and dynamics.

2.3 Unmanned Aerial Systems / RPAmSS

The use of Unmanned Aerial Systems (UAS) for environmental monitoring and remote sensing purposes has increased dramatically in the past decade (Watts *et al.* 2012). When compared to manned airborne surveying methods UAS have advantages in terms of their ability of low altitude flights and the resulting higher resolution imagery captured. Furthermore UAS offer higher flexibility due to their operational readiness and higher weather independence. Unmanned Aerial Vehicles (UAVs) as a platform can host a multitude of sensors, ranging from multispectral sensors, small scale LiDAR units, meteorological sensors, thermal sensors to recently developed hyperspectral sensors (Zhou *et al.* 2009). The rapidly developing technology in UAS has great potential for revolutionizing natural science observations similar to those transformations that GIS and GPS brought to the community two decades ago (Watts *et al.* 2012).

The current research and development project RPAmSS at the Carinthia University of Applied Sciences evaluates the potential of a “Remotely Piloted Aircraft multi Sensor System” for the fast and high-resolution capture of multidimensional environmental data (rpamss.cuas.at/rpamss). The project focuses on assessing dynamic river environments and quantitative studies of meteorological and air quality data based on a multi sensor UAV platform. The “BRAMOR”, a fixed wing UAV (as seen in Fig. 1) by C-ASTRAL Aerospace Ltd. currently hosts a high resolution digital sensor for capturing RGB and NIR imagery and an array of meteorological sensors. Furthermore the RPAmSS can be equipped with “the world’s smallest and most lightweight hyperspectral camera for UAVs” (www.rikola.fi). In the course of the project multi-temporal imagery has been captured and point clouds were derived photogrammetrically containing multi-spectral (RGB-NIR) point coloring. These datasets are in the main focus of the current study.



Fig. 1 The C-ASTRAL Bramor UAV taking off at the Feistritz study site. The fixed wing platform is launched by catapult and auto piloted during the entire flight by communication to the ground station, which is visible on the right.

2.4 Point Clouds

In general a point cloud is defined as a set of points in a three dimensional coordinate system, where every point is defined by X Y Z coordinates (Otepka *et al.* 2013). The entity of points in a cloud is most often intended to function as model for physical world surfaces and three dimensional shapes. The point cloud data exhibits the characteristics of the applied measurement method. Point clouds are mostly generated by scanning an existing scene whereby the sensor determines whether features can be penetrated, resulting in volumetric point data or only the surface information is obtained. There are multiple approaches common in geodata acquisition, such as laser scanning, sonar, radar and photogrammetry. While every point in an acquired point cloud is a vector with the first three components fixed as the points coordinates it may have additional attributes stored, e.g. the intensity of a returned signal, the return pulse number or assigned color. Often point clouds are obtained primarily to derive digital surface models (DSM) or terrain models (DTM) from them. In GIS and remote sensing these are well-established formats for topographic data and benefit from a large library of fast algorithms dedicated to their analysis. However these common raster data are limited by their ability to store only on Z value for every X Y location. The derivation

of such two dimensional products hence also leads to a reduction of the original information contained in the point cloud. By interpolation of the raw point cloud data on a 2D grid position accuracy spatial resolution is lost (Lague 2014). Thus in the course of the current study the focus lies on utilizing “raw” point clouds and exploiting their three dimensional properties in regard to riverine monitoring purposes.

2.5 Point Cloud Acquisition Approaches

Point cloud data used in physical geography have a variety of sources with active sensor systems, emitting light, radar or sound pulses to measure distances as well as passive sensor systems where distance information is generated in processing. To capture the morphology of fluvial systems remotely two main techniques are common practice: LiDAR and photogrammetry. The following chapter reviews these two well established approaches.

2.5.1 LiDAR

Light Detection and Ranging (LiDAR) for precise acquisition of surfaces in digital form has seen rapid growth since the early 2000s and is go-to standard for accurate elevation data. LiDAR is based on an active sensor emitting light pulses (often laser). The time between the emission and the reception of a reflected light pulse signal is precisely measured and the distance to the object is calculated. Every returned pulse signal generates a point in three dimensional space generating a dense point cloud as the scan result. LiDAR point clouds are captured either from airborne platforms or from ground stations, also called terrestrial laser scanning (TLS). In airborne laser scanning mainly small air planes and helicopters are made use of to carry the sensor, with some recent approaches also utilizing unmanned aerial vehicles (UAV) as a platform (Wallace *et al.* 2012, Wallace *et al.* 2014). Today multiple return or full-waveform systems are commonly used, which can capture up to five return signals or a continuous return signal wave per emitted light pulse. Since the laser pulse penetrates vegetation it enables retrieval of the last pulse revealing terrain underneath it. With a multiple-return system the vegetation is mapped as true three dimensional model, useful for metric calculations such as canopy height and volume estimations. The full waveform analysis of LiDAR data hence gives us the ability to evaluate the three dimensional structure of features above ground, given that the signal penetrates the feature. Due to the high cost involved in LiDAR sensors and acquisition methods it is seldom used for frequent mappings, especially in respect to fluvial studies.

2.5.2 Photogrammetry

Point clouds, however may also stem from passive sensors using photogrammetric approaches with overlapping nadir-looking or oblique imagery. The underlying principle for retrieval of three-dimensional information from imagery is triangulation, similar to the way humans estimate the distance to an object based on stereo vision. Photogrammetry reconstructs 3D scenes by matching conjugate points between images taken from different viewpoints. With developments in advanced computer vision photogrammetry has been undergoing a methodological revolution over the last decade. While traditionally the exact camera position and ground control points were essential to generate 3D models from imagery today's image matching algorithms eliminate the need for that. This fairly new approach is commonly called Structure from Motion photogrammetry (SfM). It differs from traditional photogrammetry mainly in two aspects. Points can be identified and matched in imagery at differing scales, viewing angles and orientations, which is of particular benefit when small unstable UAV platforms are considered. Secondly, the collinearity equations used in the algorithm are solved without information of camera positions or ground control. The data produced with the SfM-photogrammetry approach are dense, arbitrarily scaled point clouds. To transform the point cloud to map coordinates and correctly scaled elevations, desirable for use in earth sciences, two methods can be applied. The SfM algorithm not only computes the 3D coordinates of the surface but also the camera location and orientation. If high accuracy geographic coordinates and orientation of the camera are known from a real time kinematic GPS (RTK) and inertia measurement unit (IMU) they can then be assigned to the tie points created during the initial image alignment stage. Likewise surveyed ground control points (GCPs) that are identifiable in the imagery can be used to georeference and scale the reconstructed scene.

Multiple software packages integrate SfM-photogrammetry algorithms for fully automatic creation of point clouds. At the forefront of proprietary Structure from Motion solutions are Agisoft PhotoScan (www.agisoft.com) and Pix4D (www.pix4d.com). Established open-source software packages are VisualSFM (ccwu.me/vsfm), Bundler (<http://www.cs.cornell.edu/~snaveley/bundler>) with lesser known alternatives like Apero/MicMac (logiciels.ign.fr/?Micmac) and SURE (<http://www.ifp.uni-stuttgart.de/publications/software/sure>). The rapid and largely automated processing of imagery with such software package allows the reconstruction of 3D scenes for non-experts and with relatively inexpensive equipment.

However deeper knowledge about the sensors, parameters and general SfM workflow is useful to identify and minimize sources of error in the reconstructed surface.

Imagery for a SfM approach to generate 3D models can be obtained from almost any camera system. Sensors can range from consumer-grade digital cameras to professional multi- and even hyperspectral sensors. The availability of high-resolution off the shelf compact cameras with low weight makes the SfM-photogrammetry approach particularly suited for UAS applications. The low cost and flexibility of such a system makes it attractive alternative to LiDAR in particular when frequent surveys are needed. In contrast to a LiDAR approach photogrammetry does however not penetrate features, due to the passive nature of the sensor. A SfM derived point cloud therefore only represents the “seen” surface, and has limitations when ground elevation point need to be extracted, e.g. under dense canopy forest. However SfM-photogrammetry holds the advantage over LiDAR that all spectral information of the original imagery is attached to points. Since the spectral information and the point geometry both have the same imagery origin a temporal mismatch is avoided.

For the SfM algorithm to work best the identification of tie points the image acquisition should be carried out with at least 60% overlap (Kraus 2007). Depending on the focal length of the sensor head the amount of images needed to be taken in order to achieve the wanted over- and sidelap varies. A shorter focal length and hence a more wide angle lens requires less images to be taken if flight height and speed are constant. The base to height ratio defines the percentage of overlap, where the height is the distance of the sensor to the surface and the base is the distance on the surface from one image to the next. Base height ratios for a UAV SfM approach are between 1:2 and 1:5, which in turn equivalates to 60% and 80% overlap considering a 28mm focal length on a 35mm sensor camera at 100m AGL.

The imagery obtained of a scene is processed with the first step of the SfM algorithm being the identification of features, also referred to as keypoints. Such features are points that have a high probability of recognition in different images and are most likely where the texture of scene has apparent changes, e.g. corners, intersecting edges (see Fig. 2)

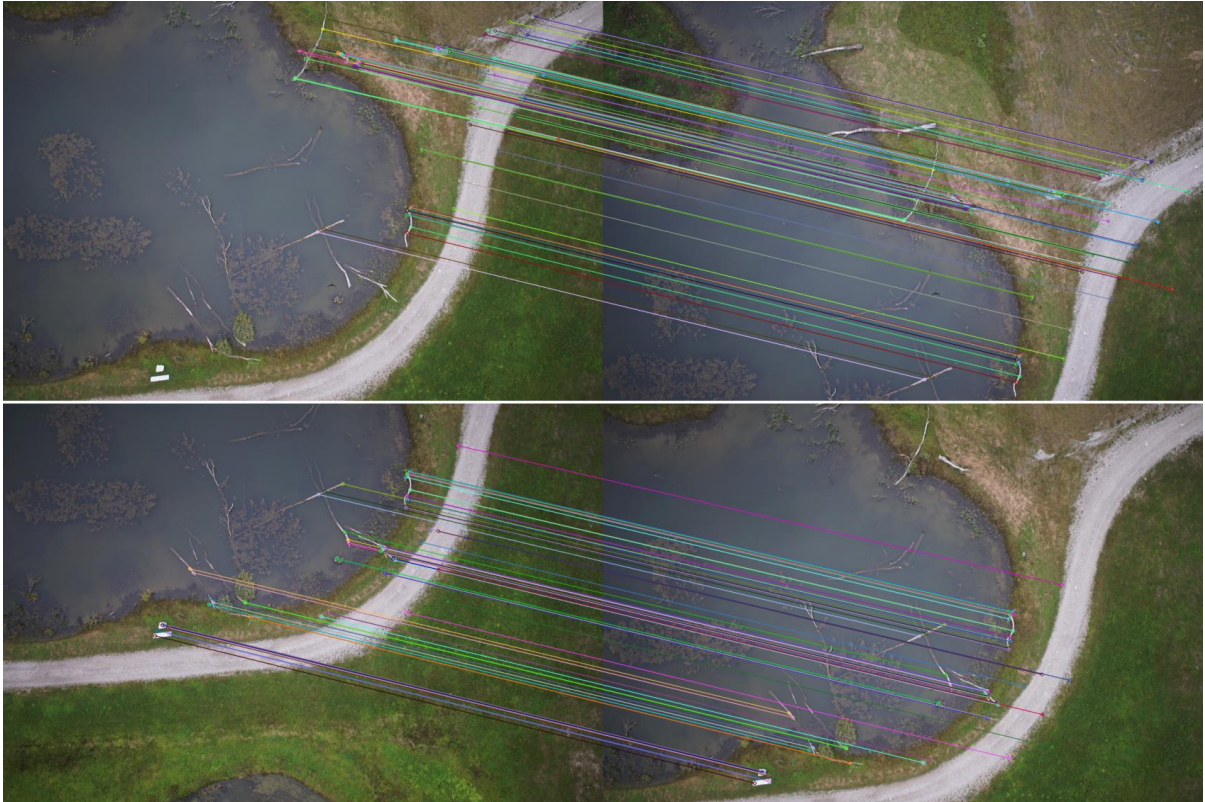


Fig. 2 Example UAV imagery (Bramor mission 02.10.2015 RGB Gail) with matched keypoints highlighted. The keypoints were identified by the A-KAZE algorithm (Alcantarilla et al. 2013) implemented in the open-source SfM photogrammetry software Regard3D (www.regard3d.org).

Common algorithms used for the identification of keypoints mainly stem from the computer vision domain. The Scale Invariant Feature Transform (SIFT) object recognition system currently is the most popular open-source algorithm used in SfM and is integrated in several software packages (Lowe 2014). Proprietary SfM solutions do not publically share the information about underlying feature detection algorithms, although PhotoScan is said to utilize a “SIFT-like” algorithm (Dandois and Ellis 2013). For every keypoint a complex descriptor is then computed in order to find correspondence of them across multiple images. Typically a filtering step follows the recognition of corresponding keypoints to discard geometrically inconsistent matches. At this stage the common keypoints of any image pair are tested for their so called collinearity, where all point that lie on a single line remain aligned in this way. The relationship between the two images is hereby specified in the fundamental matrix (F-matrix) calculated by the Eight-point algorithm (Longuet-Higgins 1981). While other methods are applicable a common approach for the evaluation of the F-matrices, hence the collinearity validation, is the RANdom SAMple Consensus (RANSAC) method (Fischler and Bolles 1981). The sampling step is the iterated until there is a 95% chance only inlier keypoints remain. The actual Structure from Motion stage starts after the keypoint filtering using only the

geometrically correct feature correspondences. Here the 3D geometry (structure) of a scene, the camera position and orientation (extrinsic parameters) and the camera's intrinsic parameters are simultaneously estimated employing bundle adjustment algorithms (Ullman 1979). Hereby bundle refers to bundles of rays connecting the camera centers to points in 3D space and adjustment refers to the minimization of a cost function that reflects measurement errors in the localization of image features in the object space, also known as reprojection errors. The minimization of the cost function concurrently optimizes the 3D structure of the scene as well as the camera parameters. Traditional photogrammetry, in contrast, requires known ex- and intrinsic camera parameters. The SfM phase outputs the camera models and poses along an arbitrarily scaled 3D point cloud, referred to as sparse cloud. In order to georeference and scale this cloud either ground control points (GCPs) with known XYZ coordinates can be used or the camera location and orientation can be exploited in case high accuracy RTK-GPS and IMU measurements are available (Smith *et al.* 2016). For high precision typically the two georeferencing methods are used in conjunction, where the camera locations are used to initialize the bundle adjustment and GCPs to further improve the solution. The incorporation of GCPs is also known to mitigate systematic errors in the reconstructed model such as the often observed so-called "bowl" effect (James and Robson 2014). Once a sparse georeferenced point cloud along with the camera parameters is obtained a typical last step in the workflow is to densify the cloud by the means of a multi-view stereo (MVS) algorithm. Hereby a densification of at least two orders is achieved. While there are many different algorithms for multi-view stereo image matching available today they all heavily rely on texture information of the original imagery. The final 3D will exhibit gaps where texture is not reliably displayed due to low resolution imagery, motion blur, over- and underexposed images or scenes with smooth or glossy surfaces. Insufficiently textured areas and patches where visibility is constrained by occlusion are filtered out during the MVS phase and result in gaps in the model. Such "holes" in a reconstructed scene, where data is essentially missing due to a lack of clear texture in the imagery, is a key restriction of a SfM-MVS approach. Provision of quality input imagery by careful consideration of texture limiting factors is hence essential for the creation of a point cloud without gaps. Hereby a well and evenly illuminated scene is critical to capture texture - analog to contrast alterations in the imagery, especially when UAS with consumer grade cameras are considered.

A LiDAR based acquisition of point clouds in comparison is also restricted in the ability to scan reflective or light absorbent surfaces (water bodies, windows of buildings etc.) though being an active sensor the illumination of a scene is irrelevant. On the contrary a SfM approach with fine texture present in high resolution imagery is capable of producing higher density point clouds when compared to sophisticated LiDAR systems (Gehrke *et al.* 2010). This applies in particular to the horizontal point density considering airborne capture of surfaces.

For any kind of point cloud based analyses and related processing methods an awareness of the differences in the acquisition of the data is crucial. Methods for point cloud classification and change detection, as presented in the following chapters, were often first and foremost developed for data originating from laser scanners. This fact will hence be taken into careful consideration when assessing results from the SfM generated point clouds in scope of this study.

2.6 Point Cloud Classification

Point cloud data is increasingly used for monitoring purposes in many sectors, from commercial surveying to scientific purposes. Applications of 3D point data range from infrastructure surveying and planning (Uddin 2002) to environmental monitoring purposes including precision forestry and agriculture (Arnó *et al.*, Moskal *et al.* 2009, Wallace *et al.* 2012). Classification of the points is relevant to the majority of the application fields. The most common example is the identification of ground points and separating them from vegetation or buildings in urban scenes. Classification of river scenes is also an important step to enable further analyses specific to field of study, such as the ground class relevant to geomorphologists. Hereby surfaces are most commonly classified based on their surface characteristics, e.g. to distinguish between fresh rock surface and rockfall (Brodu and Lague 2012). Further scientific interests, where classification of point clouds is advantageous, include grain size distribution (Heritage and Milan 2009, Hodge *et al.* 2009b, 2009a), identification of sand dunes (Nagihara *et al.* 2004) and hydraulic roughness indices of vegetation (Antonarakis *et al.* 2010). The automated classification of point clouds, however still imposes difficulties, especially when natural surfaces are considered: 1) The large amount of data representing a scene, typically with several millions of points in a set and datasets with billions of points likely to become more common as technology evolves. Such large clouds make manual classification infeasible as well as the visualization and processing of the data is challenging even for modern PCs. 2) The heterogeneity and complexity in the geometry of natural surfaces, as present in

river environments. Artificial structures such as buildings or other infrastructure typically depict of much simpler geometric characteristics than natural surfaces (e.g. sharp corners or planar surfaces) and classification of such scenes is often carried out by applying geometrical models to the surfaces, as possible with the RANSAC method (Schnabel *et al.* 2007, Huang and You 2013, Serna and Marcotegui 2014). Natural environments on the other hand exhibit vastly non-uniform characteristics at a large range of spatial scales (e.g. type and age of vegetation, variable grain size, seasonal morphological changes etc.) (Brodu and Lague 2012). 3) The variable degree of resolution (point density) and shadowing effects introduced by the acquisition method. With both LiDAR and photogrammetric point cloud generation the roughness and geometrical complexity of natural surfaces leads to some extent of overshadowed areas and possibly missing data albeit a changing sensor location. A classification method should therefore be insensitive to these areas or factoring in that data is locally missing (Brodu and Lague 2012). Furthermore spatially sub-sampling the original point cloud helps mitigate classification errors induced by variable point density.

Currently most readily available algorithms for point cloud classification label (or segment) points based on a small set of predefined characteristics, often separating only ground from non-ground points. The identification of these predefined classes is typically based on a filtering technique where few parameter thresholds define the affiliation of a point with a specific class. Common approaches can be categorized as surface-based, slope-based, morphological and multi-scale. The surface based methods (also called interpolation-based) identify ground points by assigning a weight based on the distance of each point in the cloud to an assumed (interpolated) surface. On the basis of the weights ground is separated from non-ground features (Kraus and Pfeifer 2001). Slope-based filters operate based on the local relationship between point elevation and distance between points. Often a triangulated irregular network is utilized to investigate in the local slope (Axelsson 2000). This is based on the assumption that high local slopes indicate points that do not belong to the actual terrain. A user defined threshold for the maximum local slope identifies the non-ground points. Morphological filters use dilatation and erosion based on set theory to generate opening and closing operators. Applied to a greyscale image such as a DSM, where the input is assessed in terms of spatial structure rather than numerical values (variability in grey tones), local minima can be used to refer to ground points (Zhang *et al.* 2003). Another form of filter uses a multi-scale approach where surfaces properties are classified at variable scales. Such technique is

typically applied in an iterative manner to separate feature heights from terrain elevations. Evans and Hudak 2007 introduced the Multiscale Curvature Classification (MCC) algorithm to classify discrete return LiDAR data as ground and non-ground supported by a maximum positive surface curvature threshold. The CANUPO algorithm (Brodu and Lague 2012) is also based on the multi-scale principle but can handle more complex class separation, given that multi-scale descriptors for features are created by the user by prior segmentation of the original cloud.

Results are typically stored as unsigned character in a scalar field with the header “Classification” as the standard for LiDAR data suggests (ASPRS 2011) where every is assigned a value linked to the classification value as presented in the table below.

Table 1 ASPRS Standard LiDAR Point Classes (ASPRS 2011)

0	Created, never classified
1	Unclassified
2	Ground
3	Low Vegetation
4	Medium Vegetation
5	High Vegetation
6	Building
7	Low Point (noise)
8	Model Key-point (mass point)
9	Water
10	Reserved for ASPRS Definition
11	Reserved for ASPRS Definition
12	Overlap Points
13-31	Reserved for ASPRS Definition

All classification techniques for point clouds are predominately developed for their application on LiDAR data. It is hence important to keep the differences of LiDAR generated and SfM derived point clouds in mind. A key difference is the lasers ability to penetrate (active sensor) vegetation and the resulting true 3D structure in vegetated scenes opposed to the reconstruction of visible features with a SfM approach (passive sensor). To be noted is also the fact that available software capable of classifying point clouds is first and foremost developed for LiDAR data also means that spectral information is not exploited although SfM point clouds naturally feature RGB values. Furthermore slightly moving vegetation and scenes with little texture in the imagery pose challenges for SfM based 3D modelling and can result in missing data or noise in the point cloud. Holes in the cloud can cause edge effects where misclassification occurs. Noise often present as randomly distributed points above and below

ground is identified as vegetation (if not filtered prior to classification) by most algorithms due to the similarity in 3D structure.

2.7 Ratio-based Spectral Indices

Ratio-based spectral indices are widely-used in remote sensing and GIS application that use raster images. The most known example being the Normalized Difference Vegetation Index (NDVI) which delivers evidence of the amount of chlorophyll in living plant foliage (Rouse *et al.* 1974) using spectral reflectance measurements acquired in the visible red and near-infrared regions. In the case of vegetation such index hence can be related to the plants status and health. However a raster based approach neglects the morphology of features although considering morphology and changes therein holds great potential for analyses and understanding the dynamics of nature. Calculating ratio-based indices directly on point clouds is a rarely discussed topic but has definite advantages over a 2D grid approach. The separability between features is increased and with spectral information natively being available in an image matching based point cloud acquisition approach the interpolation and reduction of the data to grid format can be omitted (also see 2.4 Point Clouds). The NDVI has been used to identify and remove vegetation from an urban environment (Maltezos and Ioannidis 2015) and in a small scale rape plant experiment to evaluate potential for estimating the NDVI's spatial distribution (Zhang *et al.* 2015). In riverine monitoring the NDVI is an important reference for identifying and analysis changes in riparian vegetation (Arneson 2015). Whereas the NDVI is commonly used to detect and inspect vegetation the Normalized Difference Water Index was originally proposed by Mc Feeters 1996 to delineate open water bodies. Both these indices may be used as tools to explore and investigate the status of rivers in-depth and to understand their dynamics better. It is hence set out to calculate the NDVI and the NDWI directly on the multispectral point clouds subject to this study. The NDVI is defined as the normalized difference between the red and near-infrared values and calculated as follows:

$$NDVI = \frac{NIR - RED}{NIR + RED}$$

The NDWI also uses principles similar to those that are used to derive the NDVI however utilizes the reflected green values from the visible spectrum instead of red:

$$NDWI = \frac{GREEN - NIR}{GREEN + NIR}$$

2.8 Fluvial Topography

In line with the “riverscape” concept described by Carbonneau and Piégay 2012, that is viewing and understanding rivers as continuous elements as part of a wider landscape with high spatial and temporal dynamics, the quantification of river topography and their associated bedforms is of fundamental interest to fluvial geomorphologists. Data reflecting the spatial and temporal heterogeneity of fluvial topography is hence in high demand though presently river science still heavily relies on field data acquisition based on simple point or line sampling. Spatially continuous high-resolution three dimensional data to quantify exposed and submerged fluvial topography offers valuable information to river science as well as management. Application areas range from hydraulic and investigations in sediment dynamics to in-stream habitat assessments and geomorphic change detection particularly of interest for river restorations (Woodget *et al.* 2015).

Apart from traditional field sampling methods there are a few common remote sensing approaches to investigate fluvial topography. Hereby quantifying submerged areas remains the most challenging part especially at fine scale. Two well-established approaches are briefly discussed here. The spectral-depth approach as passive technique and bathymetric LiDAR as active approach.

A spectral-depth approach utilizes raster imagery often obtained by aerial surveying and is the most widely used technique for remotely sensed flow depth and topography estimations in the submerged part of the channel. The method is based on an empirical correlation between the spectral properties of the imagery and water depth data acquired in the field by point sampling. Obtained correlation measures are applied to the entity of image to derive water depth estimations that can then be converted to topographic data. The maximum water depth achieved with this method is reported to be 1m (Lejot *et al.* 2007, Carbonneau and Piégay 2012). Though the method can be applied to imagery without great computational effort it requires the collection of field data near time of imagery collection. Data gathered for a spectral-depth approach are hence study site and image specific due to changing illumination of the scene and water conditions affected by turbidity and surface roughness (Legleiter *et al.* 2009, Legleiter 2012, Dietrich 2016).

LiDAR is known to deliver accurate representations of topography for exposed terrain. However, the active laser signal of typical LiDAR systems for topographic surveys is in the infrared range (1064 or 1550 nm) and absorbed by water. Quantification of the submerged

topography is hence not feasible due to lacking return signals. Though recent developments in LiDAR technology suggest great potential for obtaining underwater surface information by using blue/green signals (Kinzel *et al.* 2013), also known as bathymetric LiDAR. By using an active signal for scanning results are less influenced by turbidity and surface roughness and are hence able to obtain information at greater water depths than passive approaches. Maximum water depths of ~4m are reported for such systems (Kinzel *et al.* 2013) although shallow waters, e.g. close to the bank are known to cause bias (Bailly *et al.* 2010). Currently bathymetric LiDAR solutions to obtain data for river monitoring purposes are also still limited by availability and high cost of such systems as well as the ability to scan only submerged parts of the channel. However a recent proposal of Lague 2016 (unpublished work) introduces the use of an airborne LiDAR system that combines two separate wavelengths, 532 nm for submerged topography and 1064 nm for exposed topography of river systems (see Fig. 3).

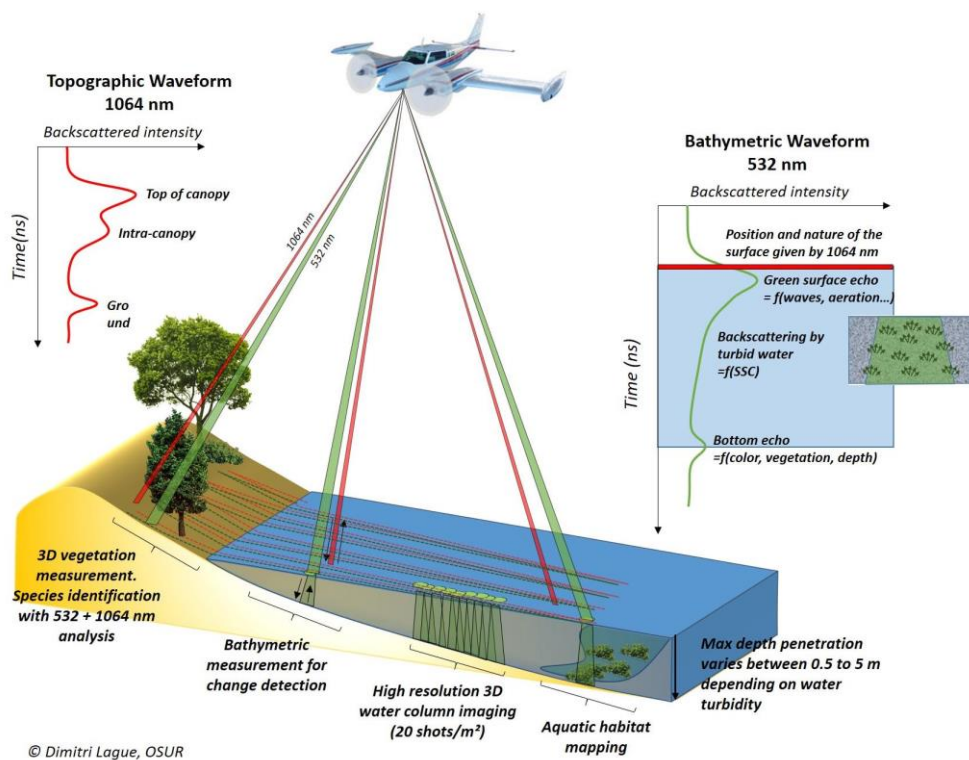


Fig. 3 Schematic representation of modern airborne LiDAR systems combining two scanners at different wavelengths. Topo-bathymetric LiDAR to quantify exposed as well as submerged riverine topography is a recent proposal by Lague 2016.

Woodget *et al.* 2015 suggest an alternative method for the quantification of fluvial topography by using SfM-Photogrammetry on high-resolution UAV imagery. They show that submerged channel parts can be accurately reconstructed provided that the water is not affected by turbidity and / or surface roughness. For clear water their study revealed maximum errors of

0.05m down to a water depth of 0.7m. These results however cannot be obtained directly from the data since the refractive properties of water need to be accounted for. Submerged data points are affected by refraction which leads to an overestimation of true bed elevation. In their 2015 study Woodget *et al.* correct for this effect by multiplying the apparent water depth with 1.34, the refractive index for clear water which reportedly varies less than 1% with altered temperature and salinity conditions (Westaway *et al.* 2001). The apparent water depth was identified by manual delineation of the river boundary manually and introduction of an assumed water surface. They based their work on SfM-photogrammetry derived DEMs of 0.02m spatial resolution and proved that fluvial topography of both exposed and submerged may be derived from the data. A SfM approach hence has an advantage over previously discussed remote sensing techniques that typically require an additional data source when both wet and dry parts of the channel are intended to be surveyed.

2.9 Comparison of Point Clouds

The comparison and identification of differences between point clouds is an essential part of their use in analysis. An evaluation of discrepancies in three dimensional properties is required for spatial error evaluation as well as for the detection of changes. Common examples of point cloud change detection in the context of river monitoring are analyses of river bank erosion (O'Neal and Pizzuto 2011), landslide and rockfall dynamics (Jaboyedoff *et al.*, Teza *et al.* 2008, Abellán *et al.* 2009), the evolution of braided river systems (Milan *et al.* 2007) or the evaluation of debris impacts on surface (Schürch *et al.* 2011).

Existing methods to compare point clouds however often require gridding or meshing. A technique as such, common to earth sciences is the DEM of difference (DoD) method. This method compares two DEMs on a pixel-by-pixel basis resulting in the measured vertical distance between them. While being a well-known and fast technique it holds disadvantages when rough natural surfaces are to be compared. Gridding a point cloud representing a complex natural scene can be a difficult task (Hodge 2010, Schürch *et al.* 2011) and it is important to realize that the information density of a derived grid decreases proportionally to surface steepness (Lague *et al.* 2013). The level of surface detail is very much limited by the DEM resolution with surfaces that exhibit different characteristics at different scales.

A method that does not require gridding or meshing of the point clouds is the cloud-to-cloud comparison (C2C). It presents a fast direct 3D comparison and is also suited for point clouds that exhibit 3D features such as overhanging parts, and hence overcomes the limitation of the

DoD technique. For each point in the source cloud the closest point in the reference cloud is obtained, the surface change is represented by the distance between the two points. The technique while being a fast way of detecting differences between clouds has limitations by being sensitive to outliers and point spacing as well as roughness.

The cloud-to-mesh (C2M) approach compares a point cloud to a meshed surface as reference (Olsen *et al.* 2010). This method is known to work well on flat surfaces however when rough natural surfaces are considered meshing the reference point cloud can be complex and introduce error (Lague *et al.* 2013). Yet, the method could be applied when comparing a point cloud to a meshed reference DSM converted to a TIN, to obtain large scale surface changes.

A method that allows for identification of differences in complex natural topographies is the Multiscale Model to Model Cloud Comparison (M3C2), recently introduced by Lague *et al.* 2013. The approach does not require gridding or meshing of the point clouds that are intended to be compared. It is robust to rough natural surfaces by computing the distance between clouds along the normal surface direction and a confidence interval is computed for every measured distance taking surface roughness and registration errors in consideration (Lague *et al.* 2013). A local measure of cloud roughness and point density is used at every step of the calculation, making the method well suited for natural environments, such as river environments. In a case study by Lague *et al.* 2013 M3C2 was successfully used on TLS acquired point clouds of the Rangitikei canyon, New-Zealand, where geomorphological changes were obtained down to 6mm at 95% confidence.

3 Methods

3.1 Study areas

The RPAmSS project currently has two study sites in scope. Both study areas are located in Carinthia, Austria and depict a river scene (see Fig. 4). Flights are carried out at a particular section of the rivers Gail and Drau respectively. The sections have been subject to the LIFE-Project, a river revitalization program within the framework of the EU LIFE-Nature conservation. The LIFE-project aims at protecting valuable riverine flora and fauna better while improving flood protection. The plan of combining nature conservation and sustainable flood protection has been realized with the LIFE Upper-Drau project officially ending in 2011 and the LIFE Gail project in 2014. To monitor the development of the study sites in all aspects

the RPA_mSS project approaches the matter with high-resolution multi-dimensional data capture. Following the characteristics of the two study sites are described in more detail with smaller scale maps given for visual reference in Fig. 5.

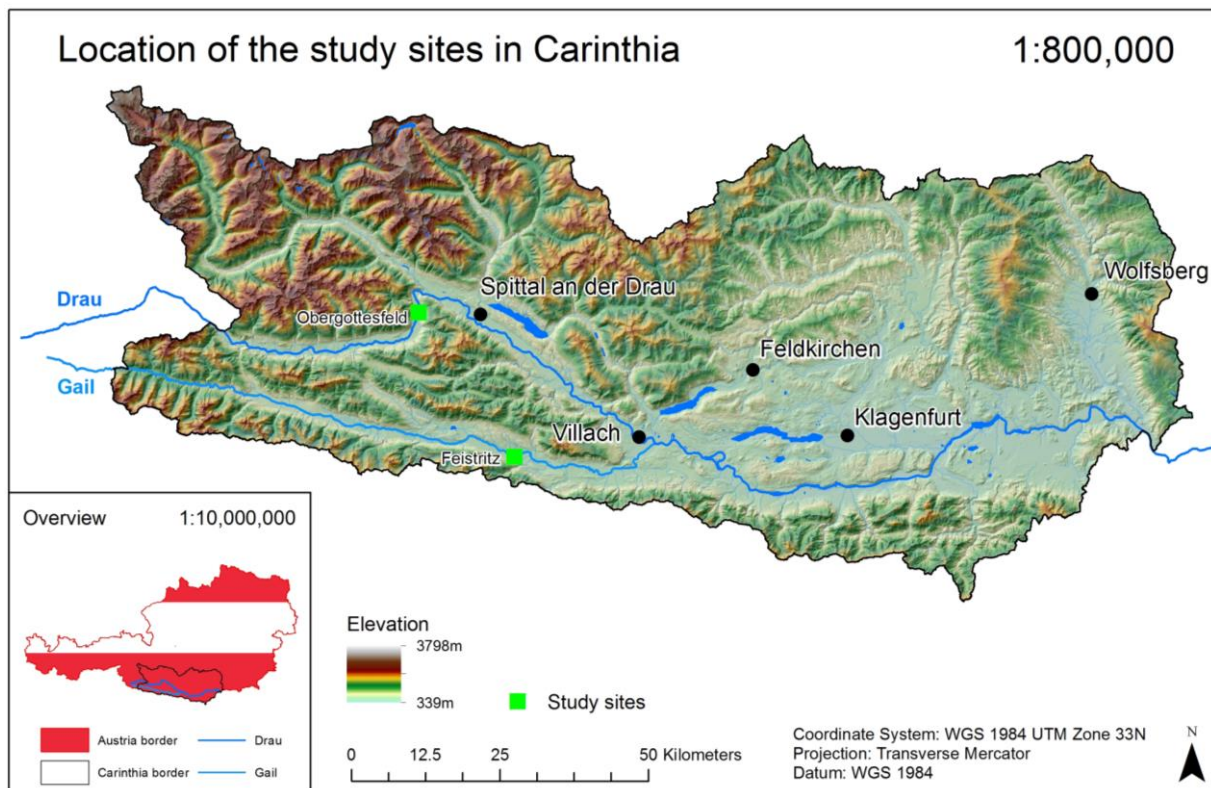


Fig. 4 General overview of the study site location

The project site at the Upper-Drau is located in the area of Obergottesfeld, Austria (560m ASL). Apart from being addressed by the LIFE project Upper Drau it is also defined as NATURA 2000 nature protection site. The area features the oldest Grey Alder forest in Austria and is host to endangered plant species such as the German Tamarisk or Dwarf Bulrush. Furthermore over 140 species of birds, including 51 red-listed species and 19 native fish species were located (BMLFUW 2011). In the course of the LIFE project the river bed of the Drau in Obergottesfeld was widened and standing bodies of water were created. These measures are aiming at creating new habitats for flora and fauna while at the same time stabilizing the river bed and reducing the hazard of floods. In order to quantify the improvements over time the area is remotely monitored with the RPA_mSS, covering approximately 3.5km².

The second study area is located close to Feistritz at the river Gail (550m ASL). As mentioned before the site is also part of the LIFE conservation project and also received NATURA 2000 status. Previously the section of the Drau was lacking ecological diversity and due to the high sediment transportation and deposition high costs for flood protection had to be covered.

With the remodeling of the Drau river bed and the construction of groynes as well as construction of still water bodies during the LIFE project habitats were improved quantitatively and qualitatively. Furthermore flood protection was enhanced by directing the river environment back to a more natural morphology (BMLFUW 2014). The study site currently is covered by RPAmSS flights over an area of approx. 0.9km².

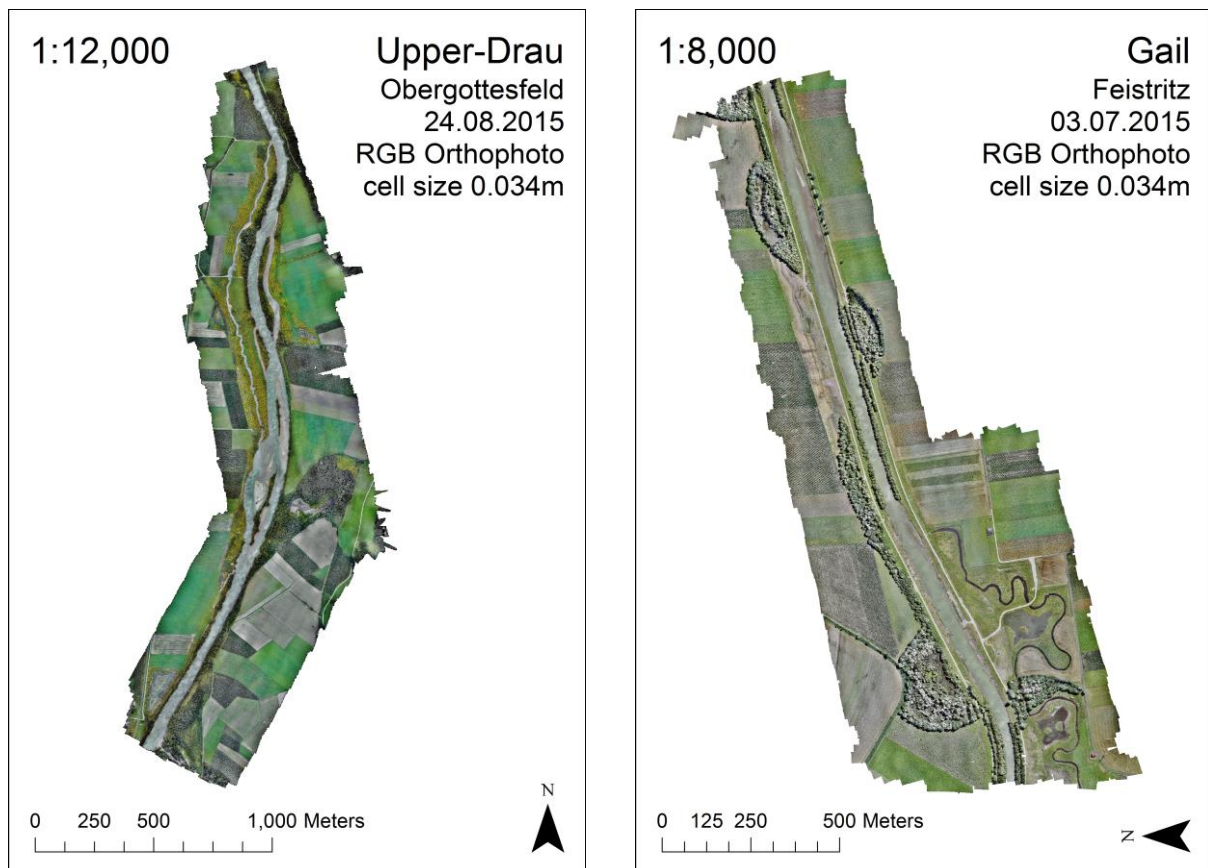


Fig. 5 Orthophoto overview maps of the two study sites based on Bramor missions flown in summer 2015.

3.2 Geodata Sources

For both of the previously described study sites multiple RPAmSS flights have been carried out and are still being carried out. Relevant to this thesis are the flights where imagery is acquired from which point clouds are then photogrammetrically derived. The system is currently able to capture high-resolution images with RGB as well as NIR information. To do so the BRAMOR is doing two consecutive flights, first equipped with a regular digital camera and then with the same camera model though modified for capturing NIR wavelength reflection. The camera used as sensor head is a consumer compact camera, a Sony a6000 with a 30mm lens, capable of taking images at 24.4 MP with its APS-C sized sensor. With a typical flight height of 100m above ground level the imagery depict of ground sample distances below 2cm. Typically

captured at 70% overlap and 70% sidelap the images are then processed in the Structure from Motion photogrammetry software PhotoScan by Agisoft to create high density point clouds and geometrically corrected orthophotos. PhotoScan aligns the imagery based on an image matching algorithm to create a sparse point cloud of tie points. The point cloud is then densified in a subsequent process. Computational results are influenced by the quality of the input imagery as well as the user defined settings for PhotoScan, an example for different depth filtering options is given in Fig. 6.

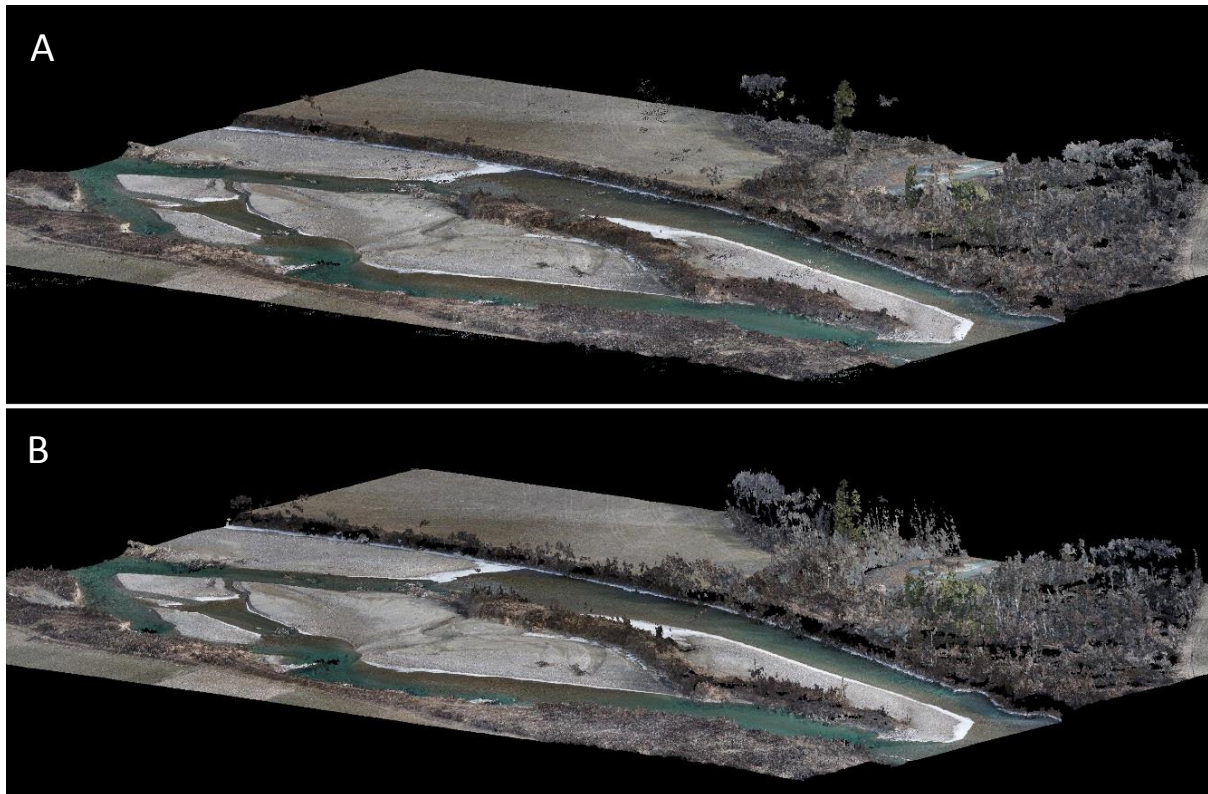


Fig. 6 Subset of the Obergottesfeld study site processed in PhotoScan at high accuracy dense cloud creation with different depth filtering modes. A) Aggressive depth filtering [114 mio points], B) Mild depth filtering [111 mio points]. Aggressive depth filtering yielded more points than the mild setting yet there is visibly more information in vegetated areas.

The current study seeks to utilize the georeferenced point cloud products from the RPAmSS, high density multi-temporal point clouds of both study sites with RGB and NIR information mapped to the points, in order to evaluate their potential for classification and change detection. Additional reference data depicts of DEM and DSM datasets of the study sites, which were obtained by airborne laser scanning in 2006 with a spatial resolution of 1m. The point cloud derived orthophotos will also be used to gain better understanding of the morphology represented in the point clouds as well as for specifying training areas for the classifier. Furthermore the orthophotos from the RPAmSS will aid as guidance for visual interpretation of respective results.

3.3 Concept

This chapter will give an overview of the general methodology of how the study is performed. The main objectives undertaken are the preprocessing of the point clouds, followed by an evaluation of the classification and ground filtering methods. Subsequently the calculation of spectrally derived indices on SfM is tested and fluvial topography is estimated with particular respect to submerged part of the channel. All applied methods and retrieved results are discussed and validated using methods like the M3C2 algorithm presented in 2.9 Comparison of Point Clouds.

Prior to the preprocessing step point clouds are derived from the RPAmSS imagery, which is not subject of this study. Currently available readily georeferenced point clouds with RGB and NIR information serve as the main input. Preprocessing of the point clouds includes the transformation to projected coordinate system as well as a check for alignment. Further preprocessing steps are the subsampling, referencing and the filtering of noise. Preprocessed point clouds are then in used to examine various classification and ground filtering algorithms. The multispectral properties of the data are exploited by the calculation of spectrally derived indices such as the Normalized Differenced Vegetation Index, a popular measurement in remote sensing. The point clouds are also examined for their ability to represent fluvial topography which is the most basic descriptor of geomorphology. The underwater topography is hereby quantified with specific focus on the refractive properties of water.

For all obtained results visual interpretation including expert opinion is conducted. Output point clouds are validated by comparison to reference data and calculation of respective spatial errors. Hereby findings are discussed with regard to their suitability for river monitoring purposes.

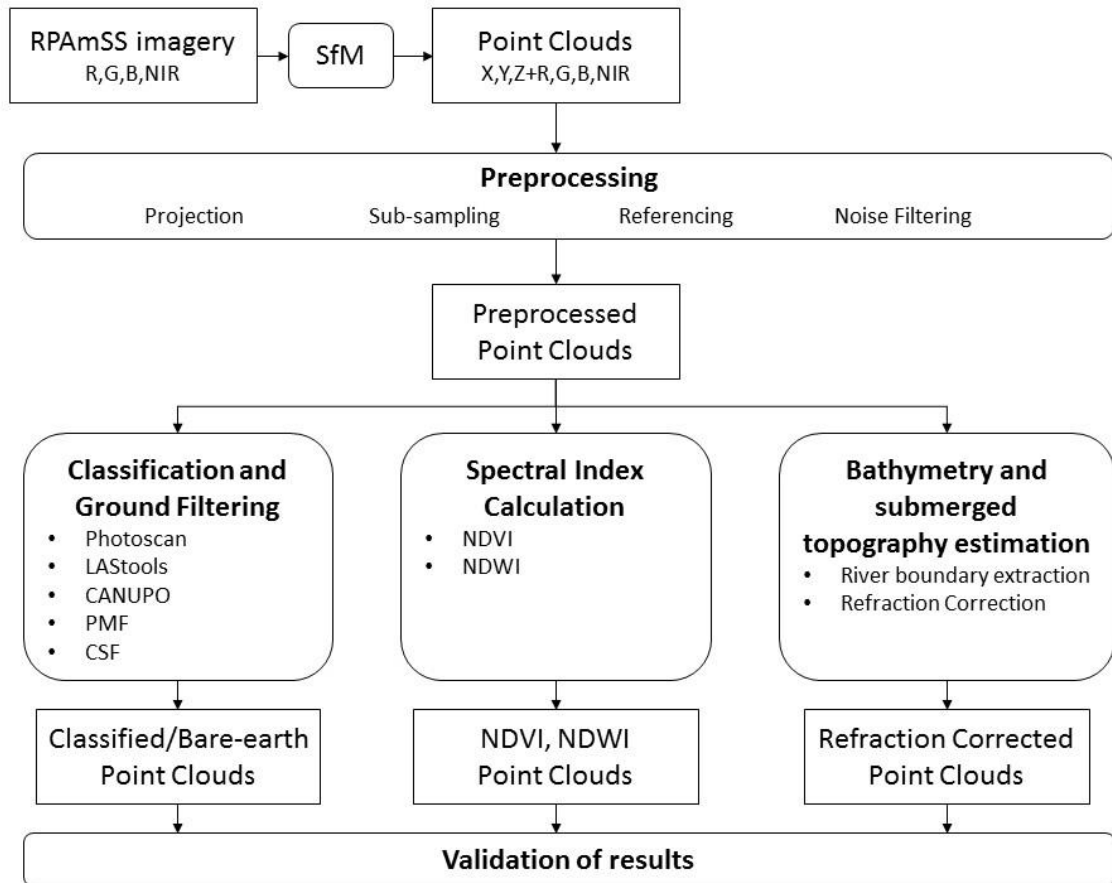


Fig. 7 Overview of the methodology. Input data given as rectangular boxes and processing steps as rounded boxes.

3.4 Preprocessing

Preprocessing of the SfM derived point clouds makes for a substantial part of the study. Data is hereby prepared for use as input in the analysis of the two study sites. Firstly the point clouds were transformed to a projected coordinate system to enable the calculation of neighborhood based measures which are often utilized in algorithms for point cloud processing.

To reduce file sizes and to normalize point densities a suitable sub-sampling approach was determined and applied to all available datasets from the RPAmSS project. The horizontal as well as vertical point densities of SfM generated point clouds can be far higher than conventional LiDAR data, especially when low-flying UAS are concerned. The large data volumes, with clouds often reaching 10^8 points and sub-centimeter point densities, not only imposes computational challenges but induces uncertainty due to difficult validation at such fine scale. Sampling of point clouds in general can have a number of advantages, with most prevailing ones being: less processing time, normalization of point densities and the removal of duplicate points. Latter being a common effect of overlapping and uneven scan patterns in

airborne laser acquisition. A sampling approach, while advantageous for stated reasons has to be chosen with care towards planned processing steps and derivative products as well as to preserve fundamental features in the cloud. The ideal sampling method can be also scene dependent, where different methods should be chosen for urban environments with many planar shapes (e.g. building walls and rooftops) and natural scenes with dispersed points representing forms of vegetation (e.g. branches of trees).

Reducing the point densities of the SfM derived point clouds of the two study sites enables creating workflows, exploring methods for point cloud classification and topography estimation while still using the full spatial extent. The reduced file sizes simplify those processes in particular that require the user to define multiple parameters manually and algorithms have to be repeated many times to find an ideal solution. This is especially true for those point cloud processing tools designed to work with LiDAR data which are applied to the SfM point clouds subject to this study.

The sub-sampled versions of the clouds were used as basis for fine alignment to the location of surveyed ground control points and hence referenced to their absolute position. Between acquisition dates systematical shifts in horizontal as well as in vertical direction are present amongst all given point clouds. These errors lead to a misalignment between the SfM point clouds and the actual surface when considering the available DTM as reference. As an example an error of 4m horizontal and 2.2m was identified when comparing the Feistritz 02.10.2015 NIR data set against the LiDAR derived DTM (considering only areas not affected by geomorphic changes introduced in the river restoration project). It is not entirely clear where the origin of these geometric errors lies. However it is assumed that relying solely on the RTK determined position and IMU derived orientation of the UAV (coordinates attached to imagery) in the generation of the point clouds caused the existing shifts. The inclusion of ground control point information during the bundle adjustment phase of the SfM algorithm is known to mitigate such errors (James and Robson 2014). A hybrid method where camera locations along with the three rotation angles are used to initialize the alignment of imagery and external GCP locations then further refine the model is commonly used and recommended (Fonstad *et al.* 2013b, Dietrich 2016, Smith *et al.* 2016) although not applied in for the RPAmSS data used for the current study. Manual referencing was hence required to allow for quantitative comparison of the point clouds to reference data.

As a last step in the preprocessing stage noise points were filtered to exclude false points from subsequent processing. The ability to reconstruct a scene with a Structure from Motion approach is very dependent on the quality of input imagery. Distinct texture, equivalent to contrast differences in the imagery is essential for the identification of tie points (see also Fig. 2), the creation of a geometrically correct dense point cloud and hence any further derivatives such as a TIN or DSM. However some natural surfaces have properties that display little texture. Particularly critical are smooth, reflecting or shadowed areas in the scene where multi-view stereo algorithms often fail to produce accurate detail. As mentioned before such patches are filtered in the MVS phase, however points that represent noise can remain. These false points are often present as low noise below the actual ground surface but can occur above and around features also. Further factors that can evoke geometrical noise in the model are motion blur, rolling shutter, shallow depth of field and image noise. While some SfM software packages, like the utilized PhotoScan can filter such noise by assuming the scene is of mainly planar, connected features (“Depth Filtering”). When reconstructing natural scenes this method will however remove valid points that belong to the finely structured surface of vegetation. The point clouds subject to this study are generated with moderate depth filtering applied in PhotoScan and do show some level of noise, in particular in the area of water bodies. Some noise is represented as sparse clouds of points and easily filtered by application of a statistical outlier filter by computing the mean distance from each point to all its neighbors and removing those with few neighbors based on the mean distance plus a number of times the standard deviation (multiplier typically defined by the user). However most scenes also suffer from noise below the ground surface where points are clustered at high density. These often isolated clusters are not identified as noise by the previously described statistical outlier filter. As a part of this study a noise filtering workflow consisting of three stages was developed and applied to the point clouds. The approach labels noise points with the class value 7 (ASPRS 2011) which enables the exclusion of them for further processing and analysis.

3.5 Classification

In the current study four different classification techniques shall be evaluated for their potential to classify the SfM derived point clouds of the river scenes. The following paragraph is intended to give an overview of the general principles that underlie the classification methods applied here. A summary of the algorithms is given in Table 2 whereby the choice reflects some of the most common approaches as well as the availability through software

packages at hand. Photoscan and LAStools are proprietary and keep the exact functionality of their classification algorithms secret. CANUPO, the Progressive Morphological Filter and the Cloth Simulation Filter are available through open-source software CloudCompare and PDAL (PCL pipeline).

Table 2 Overview of the point cloud classification algorithms applied in this study.

Algorithm/Software	Developer	Filter description	Parameters
PhotoScan	Agisoft	Slope-based	Slope Distance to ground threshold Cell size
lasground, lasheight, lasclassify of LAStools	Martin Isenburg adapted from Axelsson	Slope-based Progressive TIN densification	Cell size Planarity for buildings Ruggedness for vegetation Distance to ground threshold
CANUPO (CloudCompare plugin)	Brodu and Lague 2012	Multi-scale dimensionality	Dimensionality based class descriptor for range of scales
Progressive Morphological Filter (PCL function)	Zhang <i>et al.</i> 2003	Morphology-based	Max window size Slope Distance threshold Initial distance Cell size
Cloth Simulation Filter (CloudCompare plugin)	Zhang <i>et al.</i> 2016	Surface-based Cloth simulation	Cloth resolution Number of iterations Distance to cloth threshold

- The developers of Photoscan do not share explicit information on the algorithms used in their ground classification module. The parameters required as input do however suggest a slope-based filter.
- LAStools features a workflow that allows for classification of ground, vegetation, buildings and unclassified features and is the only software tested that can separate more than ground and non-ground in a semi-automatic way. The software requires a three phases to reach final classification results. Ground points have to be identified with lasground, a tool which the developer (Martin Isenburg) claims is a variation of the Axelsson 2000 TIN refinement algorithm and operates on multiple scales in its latest version lasground_new. The underlying principle is hence a slope-based filter where mainly depending on two parameters: a search window and a maximum slope angle criteria. Low points are decided as ground and a TIN is interpolated among them. The TIN is simplified by the criteria at each iteration. Once ground points are labeled as such the height of objects relative to the ground surface is calculated with the lasheight tool. In a last step the lasclassify function classifies above ground objects

based on a user defined distance to ground threshold. Natural features such as vegetation are separated from buildings by ruggedness and planarity criteria.

- The CANUPO classifier segments point clouds based on a multi-scale dimensionality criterion and was originally developed specifically for natural environments (Brodu and Lague 2012). The concept behind this is that local dimensionality of features changes depending on the scale a location in the cloud is looked at. The classifier defines whether an object is more like a line (1D), a plane (2D) or whether points are distributed in volume of the considered location (3D). For a specific class this information is stored as a descriptor at multiple scales. A visual representation of how descriptors are composed is given in Fig. 8. These geometric signatures for feature categories are built in the training phase of the classification where parameter files are created by manual selection of points that represent a class. The classifier uses these parameter files to separate in a binary fashion, “one against one” (e.g. riparian vegetation and ground). A classification into multiple classes is currently not available with CANUPO and is hence to be carried out step by step which requires rigorous user input.

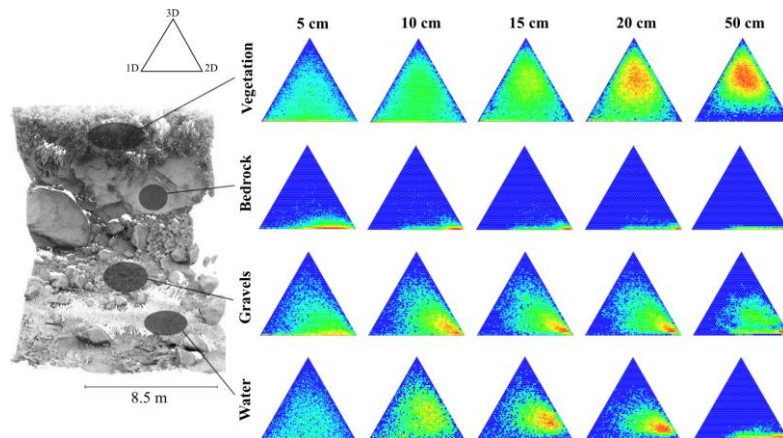


Fig. 8 Dimensionality diagrams for four classes of a river environment at different scales. The degree of clustering around a dimensionality at a given scale is colored from blue to red (Brodu and Lague 2012).

- The Progressive Morphological Filter (PMF) proposed by Zhang *et al.* 2003 uses a combination of erosion and dilatation to generate opening and closing operations to detect ground points. The filter operates in an iterative way where the user defines the initial window size that is moved through the data set and with each iteration the window size is gradually increased. Furthermore an elevation difference threshold is required as user input to determine how far away from the assumed ground surface points may be to still be counted as ground. The maximum slope angle parameter

ensures that in steep or hilly terrain ground won't be mistakenly removed. The PMF is not a classifier per se since it does not label points but rather discards all non-ground points.

- Very recently a new algorithm was suggested by Zhang *et al.* 2016 that falls into the surface-based filter category. The Cloth Simulation Filter (CSF) requires only “few easy-to-set integer and Boolean parameters” to separate between ground and non-ground features. The identification of ground points is enabled by inverting the original point cloud, turning it upside down, and draping a simulated rigid cloth over it. The user defined cell size (cloth resolution) can be interpreted as the rigidity parameter of the cloth and hence the ability to nestle in depressions of the inverted surface. Assuming the simulated cloth is the closest possible to the actual ground surface a distance threshold will classify nearby points as ground and further points as non-ground.

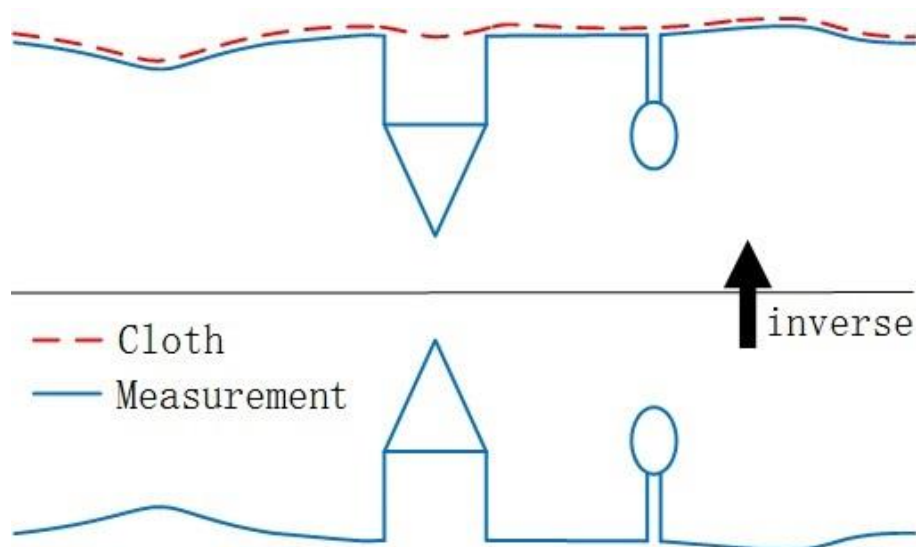


Fig. 9 Schematic illustration of the Cloth Simulation Algorithm (Zhang *et al.* 2016).

3.6 Spectrally Derived Indices on Point Clouds

To calculate two spectral indices relevant to riverine monitoring directly on the SfM derived point clouds from the RPAmSS project the data has to be prepared first. The RGB information and NIR information are gathered with separate cameras in consecutive flights. Processing the imagery in PhotoScan hence results in two point clouds, one RGB and one NIR colored. In order to obtain a ratio-based value the color information from both these datasets needs to be present on every point. To achieve a multispectral point cloud the shortest distance of every point in the NIR point cloud is calculated to the points in the RGB cloud. The NIR value is then

assigned in addition to the existing RGB values. This process inevitably requires correct absolute positioning and hence alignment of the two point clouds in three dimensional space.

3.7 Bathymetry Estimation

The quantification of the topography in submerged parts of the channel is a key interest of river science and management. The general scope of the current study lies in evaluating the potential of SfM derived point cloud data to monitor rivers in a holistic way. While it was shown by Woodget *et al.* that a SfM approach is well suited given clear water conditions their analysis was purely based on 2D grid data. Here it was tested whether a similar method they applied is suitable using the 3D point clouds from the RPAmSS project and whether the topography of the river bed can be sufficiently represented for fluvial monitoring purposes. Hereby the workflow was laid out as follows: Firstly vegetation is removed from the point cloud using a ground filtering algorithm. From the bare-earth point cloud the river boundary was extracted by spectral threshold filtering. The obtained water edge was improved by iterative thresholding of point density. Extracted elevation points at the water boundary were used to generate a 2.5D mesh across the channel, which acts as the simulated water surface. For every submerged point the distance to the assumed water surface was calculated to derive the water depth. The refraction factor of 1.34 was then applied to the apparent water depth as it was suggested by Westaway *et al.* 2001 and Woodget *et al.* 2015 (see also 2.8 Fluvial Topography and Fig. 10). The difference between the original water depth and the corrected depth was added to the elevation value of every point within the submerged part of the

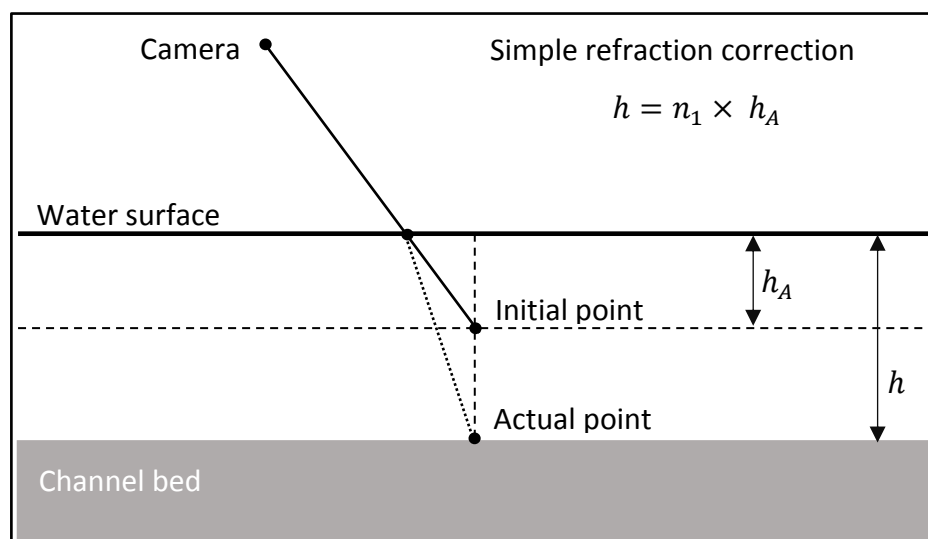


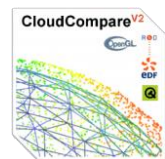



Fig. 10 Simple scheme of how data points in the submerged part of the channel are affected by the refraction of water. Applying the refractive index of water (n_1) to the apparent water depth (h_A) corrects to the actual water depth (h). Figure adapted from Woodget *et al.* 2015, not to scale.

channel. The underwater topography corrected for refraction was then merged with the exposed topography in order to generate a point cloud that may be used as basis for analysis. To examine the representational capabilities of the SfM approach based on the RPAmSS acquired imagery with regards to submerged topography the data was held against reference point samples – sonar based measurements along cross sections with approx. 20m intervals. The sonar data was gathered on the 09.12.2014 and also serves as validation for the applied refraction correction.

4 Implementation

Dense point clouds produced in PhotoScan were provided in LAZ file format, a lossless compression of the LAS format originally used for LiDAR point clouds. For every point the X,Y,Z coordinates and the corresponding R,G,B information is stored. The following table gives an overview on all software used for processing the clouds and comparison between methods.

Table 3 Overview of software used to process the SfM derived point clouds.

Software	CloudCompare  cloudcompare.org	LAStools by rapidlasso GmbH  rapidlasso.com	PDAL (Point Data Abstraction Library)  pdal.io	PCL (Point Cloud Library)  pointclouds.org
License	open-source BSD	Some tools open-source BSD others closed source. Full educational license through LASmoons sponsoring	open-source BSD	open-source BSD
Version used	2.6.3	160710	1.1.0 through OSGeo4W distribution	1.7.2 through OSGeo4W distribution
User interface	GUI, command-line	command-line, rudimentary GUI	command-line	command-line
In-/Output formats used in this study	BIN, ASCII, LAZ, SHP	LAZ, SHP, BIL, TIFF	LAZ	LAZ
Used for	Visualization, Filtering, Classification, Change Detection	Projection, Sampling, Noise Filtering, Ground Extraction, Classification, Boundary Identification	Sampling, PCL based pipeline processing	Sampling, Ground Extraction

4.1 Preprocessing

4.1.1 Projection

RTK correction data is provided in the European Terrestrial Reference System 1989 (ETRS89) by the Austrian Positioning Service (APOS). Point clouds received for the current study use ETRS89 with latitude/longitude for horizontal and meters for vertical referencing. However some further processing steps require projected coordinates since the algorithms applied rely on neighborhood functions. All clouds were hence projected into UTM coordinates (Zone 33N) using the `las2las` function of `LAStools`.

4.1.2 Sub-sampling

To find a well suited sampling approach four different methods available through the software `PDAL`, `PCL` and `LAStools` were tested. 1) `PDAL`'s decimation function is a straight forward random sampling method where every N-th point of the original data set is retained. 2) `PDAL`'s `dartsample` function identifies and discards points within a specified radius. It is initiated at a random point of the input cloud and only points that are further apart from each other than the user defined distance (radius) remain in the sub-sampled version of the cloud. It was found that `CloudCompare` uses the same algorithm in its spatial sub-sampling tool and was hence not explicitly included in this comparison. 3) The Point Cloud Library offers a so called voxel grid filter to sample a point cloud. The input cloud is hereby divided in voxels with a user defined edge length and for every voxel the centroid is added to the output cloud, therefore down-sampling as opposed to sub-sampling the data. 4) `LAStools` does not offer an explicit sampling function, however it can be achieved by combining tools. The `lassplit` tool is used to generate slices of the point cloud at defined Z intervals. The `lasthin` function is then used to place a uniform grid (edge length assigned by the user) over these slices and returns the point closest to the cell center. The thinned slices are then stacked to form the sub-sampled version of the cloud with the `lasmerge` function. This method allows for the definition of separate vertical and horizontal point densities.

To determine an adequate sampling approach for the point clouds of this study an area of the Obergottesfeld site was clipped from the original cloud (Bramor mission 03.12.2015 RGB). The sub-set shows varying degrees of surface roughness (vegetation, agricultural land, gravel road and car roof) to interpret the applicability of a specific sampling method. To ensure comparability between the results all tested sampling methods were set up to return approximately the same number of points. `PDAL`'s decimate function hereby was used as a

baseline since it naturally only accept integers. The step size 5 was chosen which reduces the original point cloud to 1/5th of points. To achieve the same amount of thinning PDALs dart sampling function was run with a radius of 6.1cm, the edge length of a voxel in the corresponding PCL tool 9.4cm. LAStools was executed with approximately twice the step size for horizontal thinning than for vertical thinning with points being discarded when closer than 10.5cm in X,Y direction and 5.5cm in Z direction.

Results of the different sampling methods were visually compared in regard to representing the scene and judged by their respective point densities (Fig. 11). PDALs decimate function noticeably degraded the structure of scene, does not normalize the point density of the cloud and was discarded as suitable sub-sampling approach. The other approaches all take the distribution of the data in consideration during the subsampling process and hence preserve structure. The voxel grid method as such however down-samples the original cloud and does not retain of the original point locations. This may be advantageous to even out variability in scanned planar surfaces, especially with larger voxel sizes, but not wanted in the context of the natural scenes subject to the current study. Furthermore attached RGB information was removed from the cloud when it was run through the PCL filter. The voxel grid sampling approach was thus not used for this study. The dart sampling method was found to be suitable for the purpose of sub-sampling the SfM point clouds. The LAStools based approach however, while also sampling the cloud on a point to point distance improves the concept since horizontal and vertical surfaces are must not be treated the same way. Sub-sampling with finer vertical than horizontal resolution allows for preserving detail in steep features while planar are also accurately represented. In other words point density increases proportional to surface variability, which results in the preservation of detail where it is most beneficial for analyses. On account of this the procedure was adopted for all original point clouds using a step size of 5cm for vertical and 10cm for horizontal filtering.

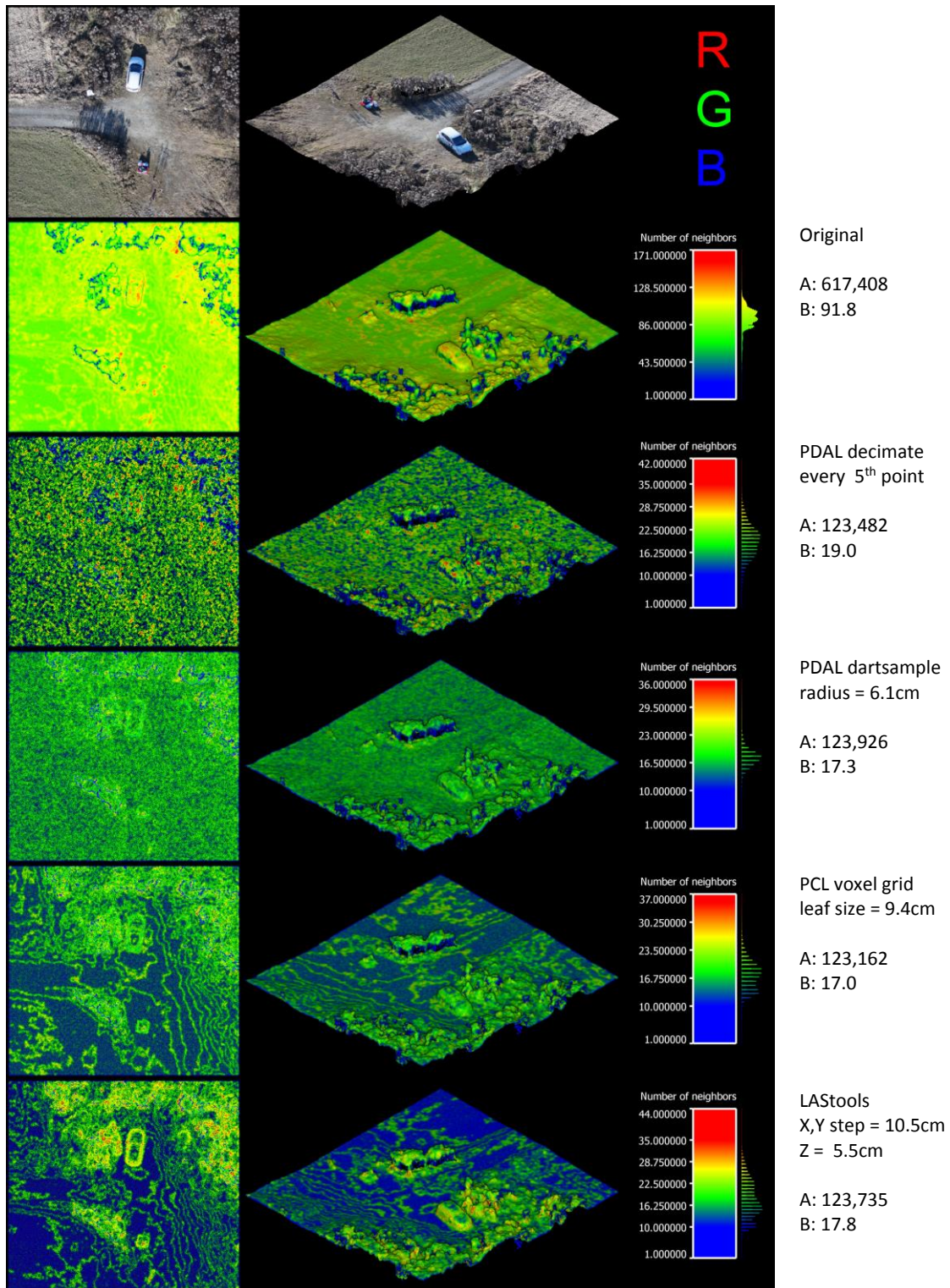


Fig. 11 Comparison of sampling methods. Point density mapped as number of neighbors in sphere with $r=20\text{cm}$. A: Number of points in cloud. B: Mean number of neighbors for $r=20\text{cm}$

4.1.3 Referencing

To enable quantitative comparison amongst the SfM point clouds as well as validation utilizing other data sources (e.g. sonar transects) the registration of the clouds to their absolute position is crucial. Since GCP targets were not laid out during every flight mission the repeated

processing of the data including GCP information in the bundle adjustment was not feasible. For analyses planned that require absolute positioning clouds were registered using the Helmert transformation (Watson 2006) which consist of seven parameters, three translation vectors (X,Y,Z), the rotation matrix (r_x, r_y, r_z) and the scale factor. To do so a point cloud from an acquisition date where GCP targets were laid out and clearly visible was chosen to be referenced to the GCP coordinates surveyed with a Leica Zeno GG03 (RTK mode with 1cm horizontal and 2cm vertical accuracy). For the Bramor mission in Feistritz on the 02.10.2015 ground targets are placed on top of the surveyed GCP locations. Four of the targets and the corner of a landmark (rock) fall within the extent of the point cloud and are identifiable and visibly stand out in the NIR data. To align these locations with the coordinates of the GCPs the reference points were imported to CloudCompare as 3D shapefile. Ideally the highest density point cloud is utilized to recognize and match the GCP locations displayed in the cloud with the reference points. Loading the original density point cloud (02.10.2015 NIR) in CloudCompare is however not feasible since the software decompresses the LAZ format and reads all points into the main memory. The file size hereby increases from the compressed 8.7GB to 23.9GB, exceeding the available RAM (16GB). To bypass the issue clipping regions were defined around the surveyed GCP locations where visible targets likely to fall within (5m radius). These regions were extracted with LAStools which offers point streaming and is hence able to process without having to read the whole file first. Within these buffers the center of the targets were then aligned with the corresponding surveyed GCP. Hereby the point closest to the center of the target was chosen by visual inspection using the raw imagery of the mission as aid (see Fig. 12). A root mean square deviation (RMSD) of 0.24m was obtained following the registration based on the seven parameter Helmert transformation.

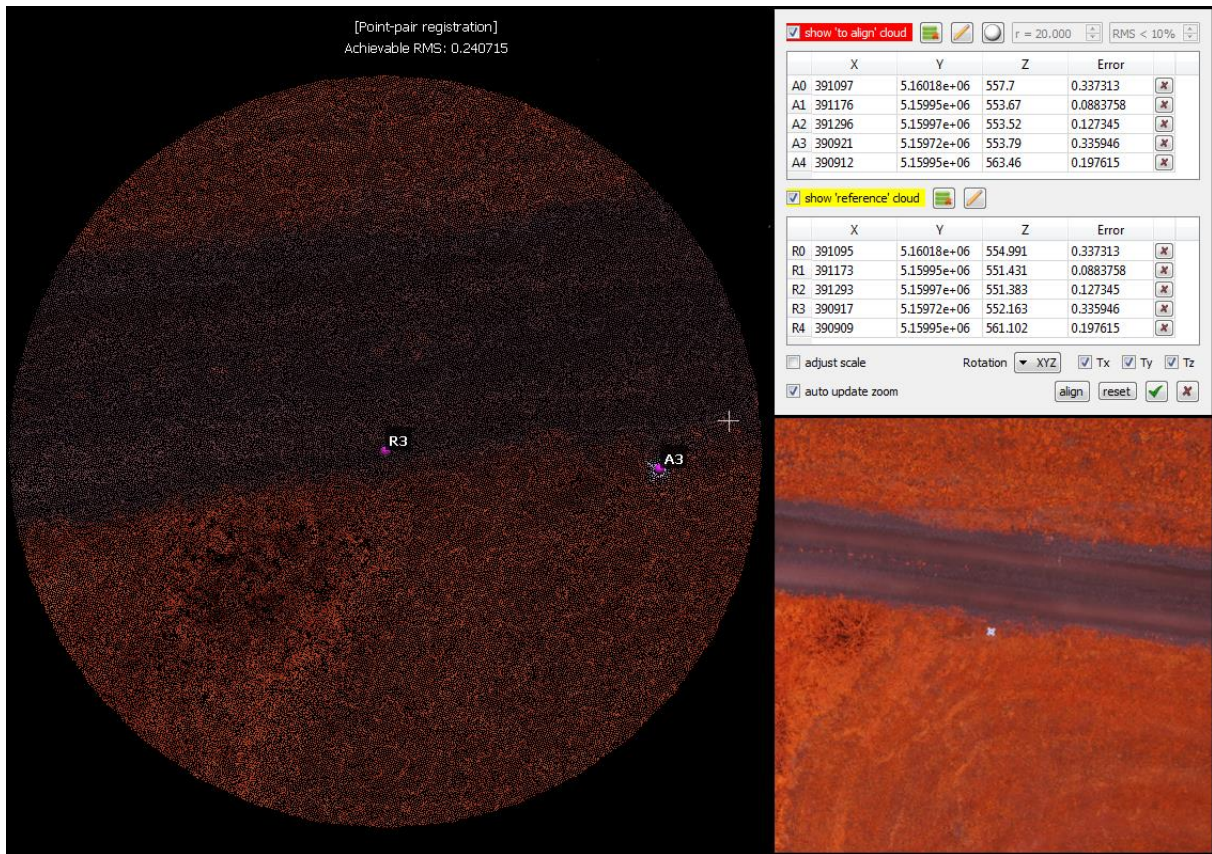


Fig. 12 Registration of the dense point cloud (Bramor mission 02.10.2015 NIR) to the surveyed GCPs. Four ground targets and one landmark corner were identified and aligned to the corresponding GCP coordinates. A root mean square deviation of 0.24 was achieved.

As a comparison the raw imagery of the same mission was reprocessed in PhotoScan with manually placed GCP markers and will be referred to as GCP point cloud. The point cloud derived with camera locations but without GCP information will be referred to as RTK point cloud. Both of the clouds were held against the DTM surface (2006 ALS) using the M3C2 method (surface normals calculated based on $r=15m$), with all vegetation and buildings removed by LAStools as described in 4.2 Classification. The manually registered RTK point cloud depicts of a RMSD = 0.76m and the GCP point cloud shows a RMSD = 1.32m (Fig. 13). Spatially presenting these errors reveals a deviation pattern towards the up- and downstream end of the GCP point cloud. A similar pattern was reported by Javernick *et al.* 2014 and referable to the lens distortion as well as the absence of GCP information towards the edges of the data. Extracting the points within the convex hull of the GCPs used for manually aligning the RTK cloud results in very similar RMSDs of 1.18m for the RTK cloud and 1.17m for the GCP cloud. The deviation of $>1m$ is due to the fact that the DTM used for reference is obtained before the river restoration began. The geomorphology has changed significantly with

anthropogenic earth displacement between the acquisition years 2006 and 2015. A comparison of the manually referenced RTK cloud and the GCP cloud yields a RMSD of 0.11m within the same convex hull (see Fig. 29).

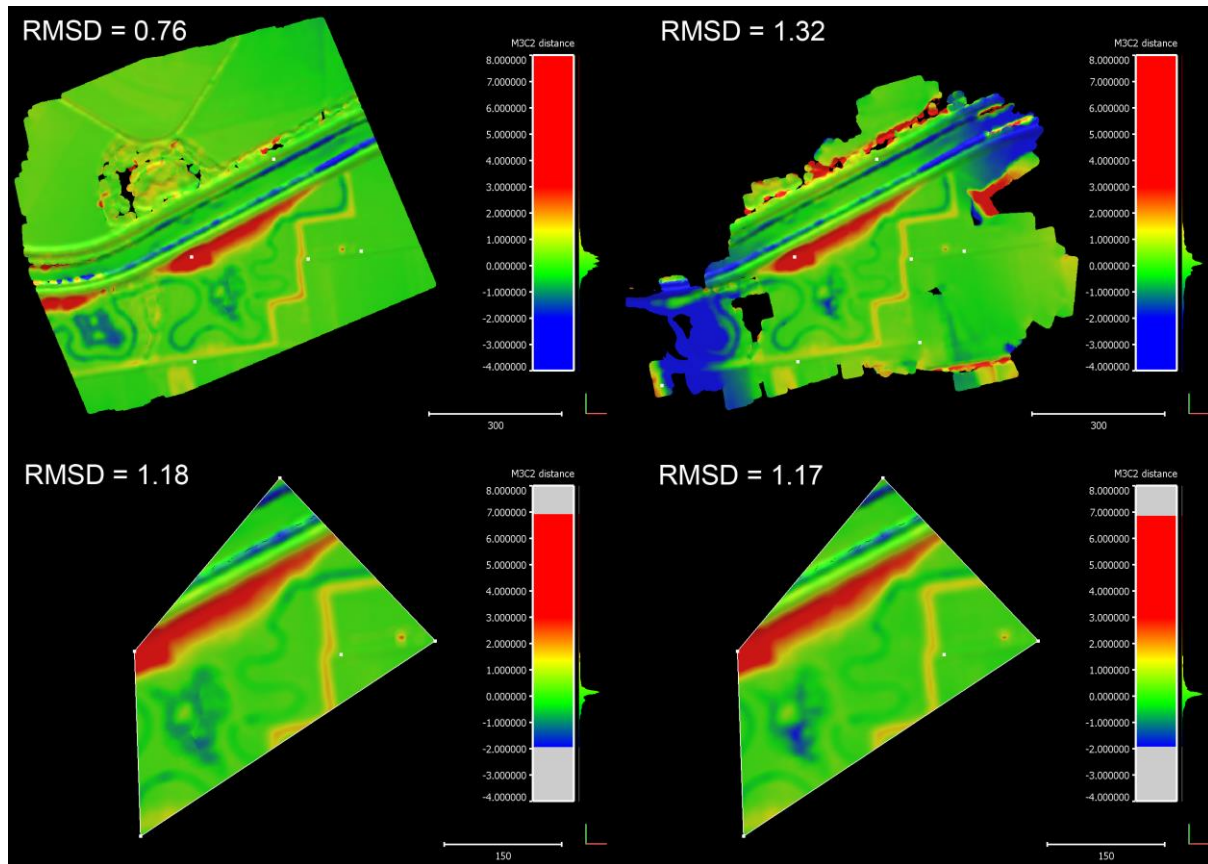


Fig. 13 Comparison of the RTK cloud (aligned to GCPs by Helmert transformation) on the left the point cloud produced in PhotoScan including the GCP information in the bundle adjustment on the right. For both clouds the difference to the DTM (2006) is shown based on the M3C2 method (surface normals calculated on $r=15m$). On the bottom the clouds are segmented by the convex hull of the used GCPs and therein depict of similar RMSD values.

The seven transformation parameters obtained from the manual alignment carried out in CloudCompare were applied to the sub-sampled version of the 02.10.2015 data set. Other clouds without visible GCP targets laid out were manually aligned to the sampled 02.10.2015 NIR cloud which thereby acts as reference. These registrations were carried out by manually picking corner points of unmovable features that are present in both sets.

4.1.4 Noise Filtering

The developed noise filtering workflow consists of three stages and utilizes multiple LAsTools functions in a batch, enabling automatic detection of noise in multiple datasets without user input. As first step the DTM (ALS from 2006) is used to label points as noise when they are far below the terrain models surface. This operation is achieved with the LASheight function which is able to read in ground points and classify any point of the input data set below a user defined threshold as a certain class number. The ALS derived DTM was converted to a point

cloud by the extraction of elevation values at the centroid of each raster cell and every point was given the classification label 2 for ground. It was defined that every point 4.5m below the LiDAR acquired surface is noise (class 7). A “closer” threshold will, in the case of the two study sites, result in the removal of valid points within the river channel and still water bodies. This is due to the fact that a SfM approach can retrieve information of the submerged topography (provided that the water is clear) while the DTM presents an assumed water surface as well as the altered geomorphology at the river banks in the course of the restoration that has taken place between the acquisition dates of the data.

For a finer detection of low noise the SfM datasets were gridded and a statistical assumption of the actual surface was performed. For the Gail as well as the Drau scene calculating the 10th percentile of elevation values within 0.6m x 0.6m grid cells and labeling points 0.5m lower than this surface model was found to give best results to identify the present low noise. The LAScanopy function, a tool developed to compute forest metrics, was used to calculate the 10th percentile raster that was subsequently used as “ground” surface in the LASheight function to label sub-surface noise as 7.

With larger artifacts below the surface classified as noise some scattered false points remain above the surface. The LASnoise function was used to flag those points as noise that have few other points in their neighborhood. A point was counted “isolated” when <10 other points are found in a 3 x 3 x 3 cell neighborhood where every cell has an edge length of 0.2 and the point in question is placed in the center of the 27 cells. These parameters were chosen specifically for the point density chosen for sub-sampling (see 4.1.2 Sub-sampling) and were found to determine most noise judging by visual interpretation. However the criteria was set in a conservative manner to avoid any removal of valid points and to make the final noise filtering script applicable to multiple datasets without the need for time costly parameter tweaking.

An example of the three step noise identification and labeling is given in Fig. 14 where noise is predominant in the still water pond area. All three types of noise filtering were set up to classify noise as 7 to enable excluding the class in further processing steps.

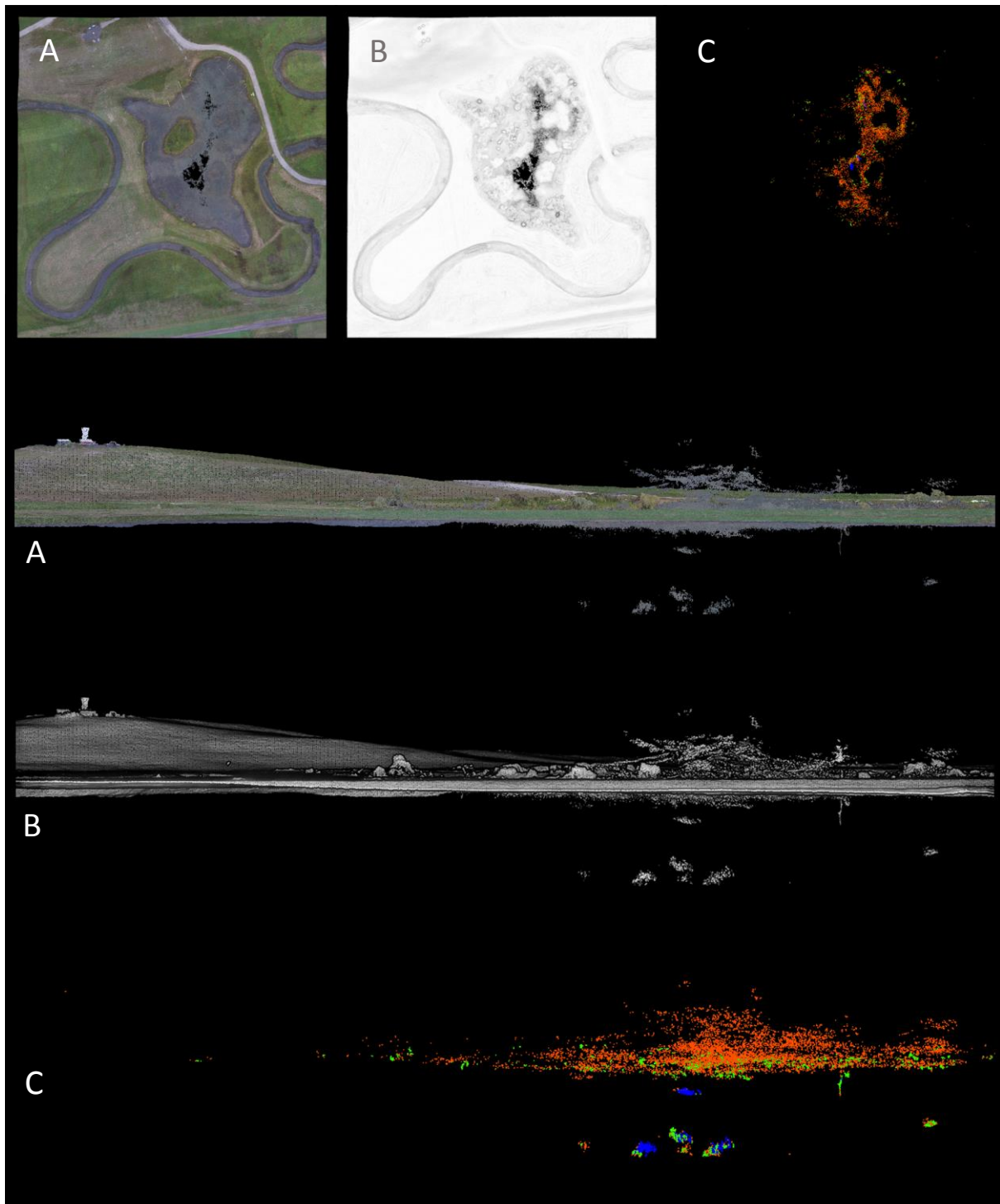


Fig. 14 Sub-set of the Gail study site (Bramor mission 02.10.2015 RGB) with still water body affected by noise. View from top and side in RGB (A), shaded (B) and identified noise (C). Noise is visualized in different colors to highlight the points labeled by the individual noise filtering steps undertaken. Blue points are 4.5m below the DTM surface, green points are 0.5m below the assumed surface (10th percentile raster) and red points are defined as isolated with less than 10 points in their 0.008m³ neighborhood.

4.2 Classification

In this chapter five point cloud classification algorithms are held against each other to evaluate suitability for SfM based river monitoring. All tested filters were applied to a sub-set of the point cloud of 02.10.2015 NIR Bramor mission in Feistritz. This specific scene was chosen for

its variety in natural and man-made features – the river, still water bodies, forest, low vegetation, dams, buildings and parked cars. The point cloud was generated in Photoscan using a high accuracy setting for the alignment process and low accuracy with moderate depth filtering in the densification. Noise points were identified and labelled as such and were suppressed for classification. Misclassification of coarse noise clusters as vegetation is thus avoided to a large extent. After noise removal the sample cloud features 14,860,798 points. Sub-sampling was not carried out for the classification experiment to find out how the various techniques deal with the variable point densities generated in SfM processing.

The previously described classification algorithms (see 2.6) were applied through the software Photoscan, LAStools, CloudCompare and PDAL. Parameters were manually set and results were visually evaluated for their classification performance. Typically 5-20 iterations with different parameters we carried out per algorithm to gain optimal results. An overview of the parameter values chosen for each respective classification method is given in Table 4. All processing was undertaken on a PC with medium specifications, an i7 3.4Ghz processor and 8Gb main memory. Where possible the point cloud was processed parallel on all 8 cores. Processing times were recorded to investigate the computational efficiency of the applied classification methods.

- PhotoScan allows for the classification of ground versus non-ground points once the dense point cloud is generated. It also classifies low noise points though they were disregarded and instead identified in a successive step with the workflow described in 4.1.4 Noise Filtering to make results comparable. The classification tool of PhotoScan was set up with a 1m cell size and maximum slope angle of 15°. The classification threshold distance to the generated ground surface was chosen at 0.5m. With the chosen setup the computation took just over 3 minutes.
- The classification with LAStools is broken into three parts / functions, lasground to identify ground points, lasheight to assign the above-ground height to every point and lasclassify to label non-ground features with vegetation and building classes. Prior to the execution of these functions the point cloud was split into tiles with 100m edge length with a 10m buffer using the lastile function. This tiling approach allowed for multithreaded processing on 8 cores, hence 8 tiles simultaneously and significantly decreases processing time. Hereby a buffer surrounding every tile causing them to overlap is essential since the lasground function utilizes a TIN surface which in would

cause edge artifacts in ground point identification between tiles. The buffer is removed and the tiles are merged once the classification was performed. The initial determination of ground points was undertaken at a step size of 25m and distance to ground threshold of 0.3m. With the above-ground height assigned to points lasclassify parameters of 0.2 ruggedness and 0.025 planarity were assigned. A larger planarity value, which essentially corresponds to the value of deviation neighboring points can have, led to misclassification as building in the forest canopy. The whole classification process including the tiling and reverse tiling of the point cloud ran in under 2min.

- The CANUPO plugin of CloudCompare does not allow for direct classification of a point cloud using for example default parameters. Contrary to the other filtering algorithms CANUPO requires the manual segmentation of training areas for two opposing classes. Hereby any two user defined classes can in principle chosen, however features that differ significantly in their dimensionality naturally work best (e.g. 2D rooftop vs. 3D forest canopy). In this case 5 training areas were segmented to represent the ground class and 5 forested areas were chosen as vegetation class. These two classes were used to train the CANUPO classifier at 8 scales, from 1m to 8m at 1m increments. 100,000 randomly sampled points from either class serve as so called “core points” and are used as basis to train the classifier. CANUPO separates the two classes by the means of a Linear Discrimination Analysis and generates a plot where the classification boundary may be manually adjusted (see Fig. 15). However the training sub-sets for the ground and vegetation class yielded a balanced classification accuracy of 99% which offers sufficient discrimination between the two classes at the chosen scales with no further modification of the boundary. The trained classifier comprising of binary class descriptors at multiple scales was saved as a parameter file. The classifier was applied to core points of the test point cloud. Core points were established by spatially sub-sampling at 0.2m point spacing which decreases calculation time and mitigates the influence of SfM owing variable point density. The classification label assigned to the 2,721,291 core points is then propagated to neighboring points in the original cloud based on the shortest distance. The classification confidence output by CANUPO was used to create a second version of the cloud at 99% confidence interval.

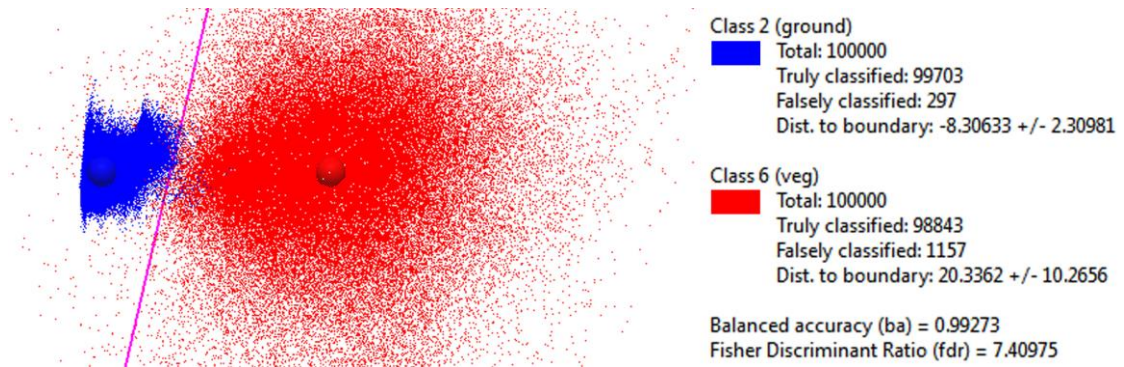


Fig. 15 LDA results of chosen training points for ground and vegetation class using the CANUPO plugin to create a classifier. Each class feature 100 000 training points and the LDA resulted in a separation with 99% balanced accuracy based on the 8 chosen scales on which the dimensionality of features is identified.

- The Progressive Morphological Filter was applied through a PDAL pipeline which allowed the LAZ input format rather than the PCD format required by PCL. The iterative algorithm was executed with 1.2m cell size, a maximum window size of 30m, 15° max slope angle, an initial height above ground of 0.3m and a maximum distance of 3.5m. The window size is grown exponentially with every iteration. The filter does not classify ground points as such but rather discards all non-ground points. Color values assigned to points in the LAZ file are erased in the PMF computation currently making the method more suited for DTM generation only. Using the PMF through the PDAL software does not allow for processing on multiple cores. The extraction of ground points hence took 32h and 21min.
- As a new development by Zhang *et al.* 2016 the Cloth Simulation Filter was included in the comparison. Ground and non-ground points of the test cloud were separated by applying the “relief” scene mode which affects the rigidity of the cloth. Furthermore a 1m cloth resolution with a distance threshold of 0.2m at 500 iterations was chosen. Executed in CloudCompare the filter uses all 8 available cores for processing and results were computed in 5sec.

Table 4 Applied classification techniques with respective chosen parameters, number of identified ground points and processing time. All processing was carried out on a PC with i7 3.4Ghz processor and 8Gb RAM. The input cloud features 14,860,798 points.

Algorithm/Software	Parameters chosen	Ground points	Processing time
PhotoScan	15° max angle 0.5m max distance 1m cell size	13,909,140	3min 11sec 8 cores
lasground lasheight lasclassify of LAStools	25m step size 0.3m ground offset 0.025 planarity 0.2 ruggedness	13,634,296	1min 58sec 8 cores
CANUPO (CloudCompare plugin)	1-8m scales 1m increments Dimensionality descriptor 99% CI cut-off	13,707,674 12,983,245	11min 32sec 8 cores
Progressive Morphological Filter (PCL function)	1.2m cell size 30m max window size 15° slope 0.3m initial distance 3.5m max distance exponential increments	13,502,797	32h 21min 1 core
Cloth Simulation Filter (CloudCompare plugin)	“relief” scene 1m cloth resolution 500 iterations 0.2m classification threshold	13,617,808	5sec 8 cores

4.3 Spectrally Derived Indices on Point Clouds

To calculate spectral indices on the point clouds of the RPAmSS project multispectral information needs to be assigned to every point in the dataset. In order to do so the RGB and NIR point cloud were combined using a shortest point to point distance approach. Prior to this process a RGB and NIR point cloud from the same mission were finely aligned using five manually chosen tie points. As an exemplary data sub-sampled versions (0.5m min. distance between points) of the point clouds from the Bramor mission 12.10.2015 at the Drau study site were used and aligned in CloudCompare with a RMS of 0.08m. Following common areas of present points in the data were determined for both point clouds. This avoids the assignment of values from far points in those areas where the RGB cloud has points but the NIR cloud exhibits missing data due to insufficient matching information in the SfM process (see also 2.5.2 Photogrammetry). The LASboundary function of LAStools was used to create polygons of the area that both the RGB and the NIR point cloud cover. The intersection of these polygons was calculated in ArcGIS and both point clouds were reduced to the remaining points that fall within this area by using LASclip. Although this process only operates on two dimensions it removes most problematic areas sufficiently. Once the “common denominator”

of points in the two clouds is found the RGB values of each band are written to scalar fields and NIR values are transferred based on the shortest distance. Hereby the NIR information is written to a scalar field of the RGB point cloud using the “Interpolate from other identity” function of CloudCompare. Storing the RGB and NIR values in scalar fields allows for undertaking the arithmetic operations between them to calculate the NDVI and NDWI. The indices are presented for the Drau study site in the Results chapter.

4.4 Bathymetry Estimation

The process to gain topography information of the submerged channel with correct elevations consists of two stages. The 1) water boundary identification and extraction and the 2) refraction correction which requires prior calculation of water depth based on a simulated water surface. The method was tested on the RGB colored point cloud from the 22.04.2015 Bramor mission at the Gail study site. Water conditions were clear on the acquisition date providing enough data points within the submerged part of the channel. The point cloud was finely aligned to the GCP based referenced data set 02.10.2015 NIR with RMS = 0.2m (see 4.1.3 Referencing) and treated with the noise filtering method described in 4.1.4 Noise Filtering. Vegetation was suppressed by a LAStools based classification of the cloud, retaining only the ground and the unclassified class (see Fig. 16). Finally the main part of the channel was extracted by coarse manual segmentation along the banks in order to focus on the relevant submerged riverbed and to reduce file size. This prepared point cloud was subsequently used for extraction of the water boundary and refraction correction procedure.

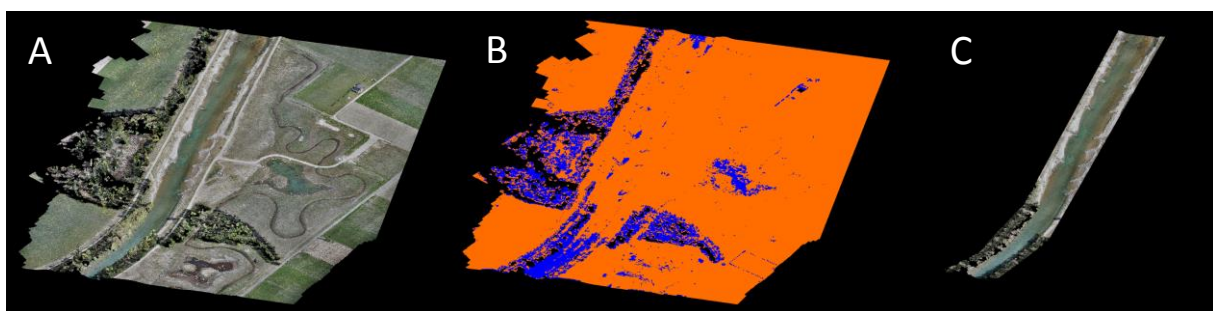


Fig. 16 Preparation of the 22.04.2015 RGB point cloud of the Gail study site for bottom topography estimation. A) Oblique overview in RGB, B) Filtered ground (orange) and unclassified (blue) class and C) manually segmented main part of the channel.

4.4.1 Water Boundary Extraction

In order to obtain water depth values for all submerged points in the cloud a simulated water surface needed to be introduced. Woodget *et al.* obtained a water surface by manual selection of elevation points along the waters edge followed by interpolation between these points. In the current study the edge of the water was extracted by threshold filtering of the RGB

information stored on the points. In the case of the 22.04.2015 data only the blue band was used to filter a rough river boundary that was then further refined by point density threshold filtering. The 0-255 scale of the blue band was cut off at 100 to drop most points in the river bank that do not contain as much blue information as the water (Fig. 17). Points in the river bank that remained due to some level of blue color were then filtered based on the volumetric point density in these areas. Since the threshold for the blue band removed at least some points in their neighborhood the areas outside the water boundary depict of lower point densities. To further refine the edge of the water the volume density was calculated on all points using an iterative approach based on descending search radii. Volume density is hereby defined as number of neighbors divided by the neighborhood volume:

$$Volume\ density = \frac{N}{\frac{4}{3}\pi r^3}$$

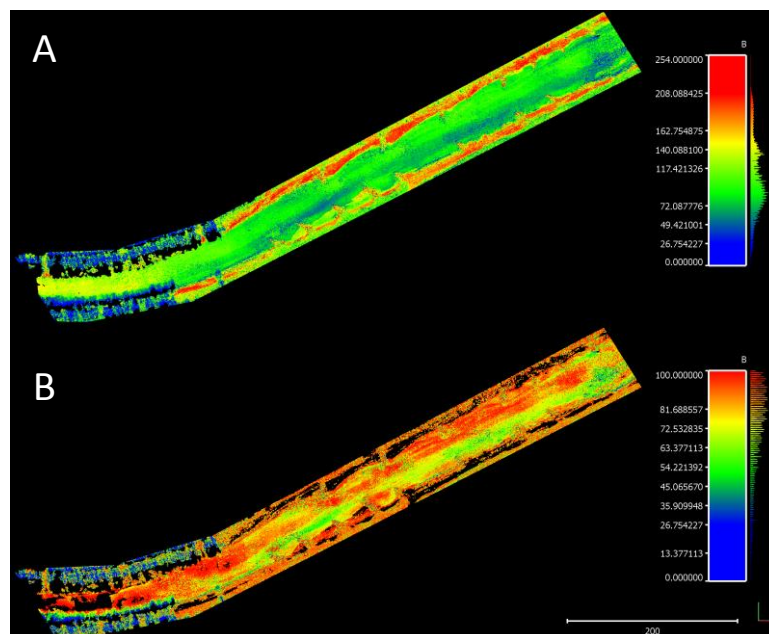


Fig. 17 Threshold filtering of the blue channel information to eliminate most non-water points at the boundary. A) The unfiltered blue band and B) the filtered point cloud with cut-off value 100 at the bottom.

The exemplary dataset was treated with volume density based filtering using 2m, 1m and 0.5m neighborhood radii, delivering an estimation of the water boundary (Fig. 18) that required minimal manual cleaning (1min). The extracted submerged area of the channel was segmented to discard the upstream section of the Gail where imagery was heavily affected by tree shadows (see Fig. 17).

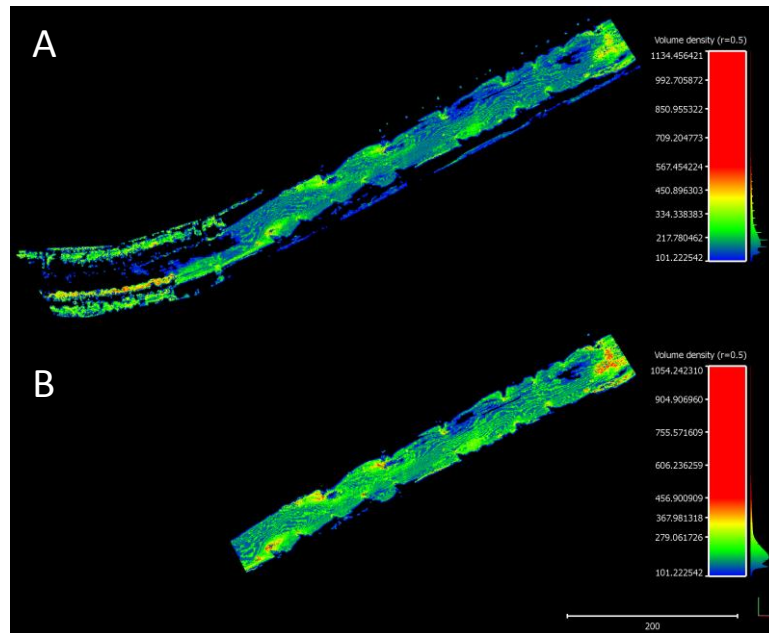


Fig. 18 Volume density based threshold filtering to refine the water boundary. A) Final filtering step with 0.5m search radius and lower cut-off value of 100 applied and B) the manually segmented section of the channel that is not affected by shadow.

Finally the water boundary is generated as shapefile using the LASboundary function of LAStools with the concavity parameter set to 1m (Fig. 19).



Fig. 19 Extracted water boundary for 22.04.2015 dataset of the Gail study site.

4.4.2 Refraction Correction

In order to correct for refraction the water depth was calculated for every point in the submerged part of the channel. To do so a water surface was introduced by interpolating between elevation values at the edge of the water. The elevation values were extracted within a +5cm buffer of the water outline polygon from the original point cloud by LASclip. A 2.5D Delaunay triangulation served as interpolation method across the channel.

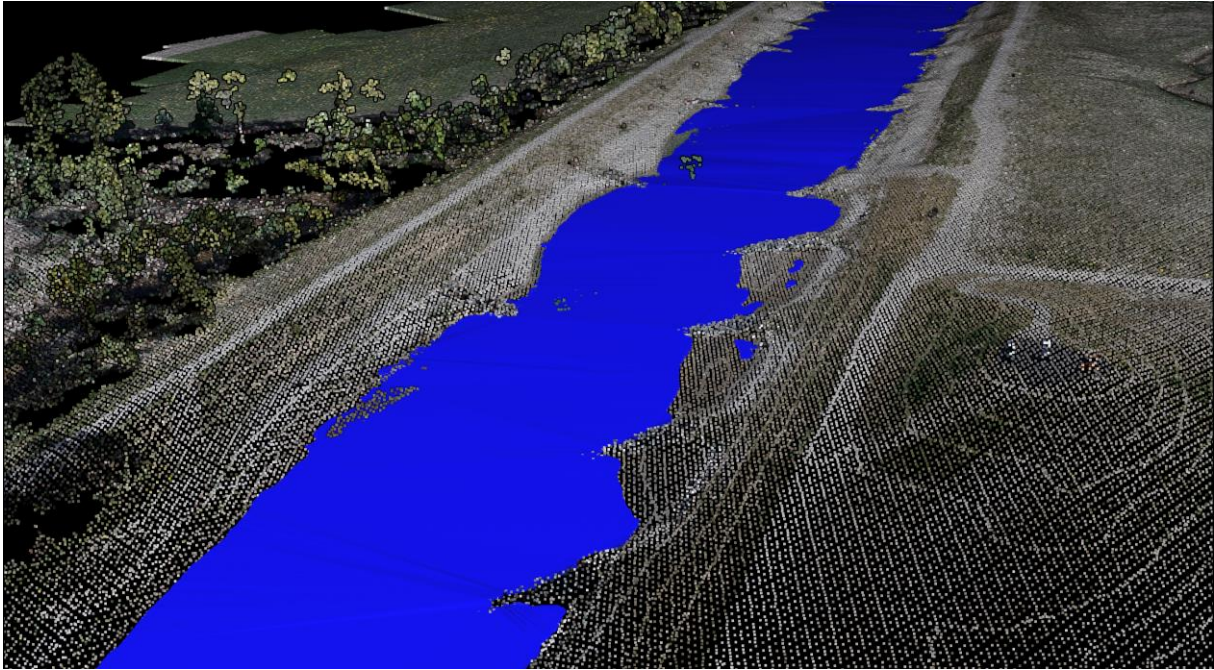


Fig. 20 Oblique view on simulated water surface mesh.

The distance of submerged points to the mesh were calculated with the C2M method and stored on the points as estimated water depth values. Water depth was then multiplied by 1.34, the refractive index of water. The difference between the un-corrected water depth and the refraction corrected water depth was added to the elevation values of submerged points. An overview of the channel section with corrected water depth values is given in the results (Fig. 25).

5 Results

5.1 Classification

Classification results of the methods applied are visually presented in Fig. 23. Specific focus was laid on the ability to detect ground points since it is the most sought-after information that can be derived from point clouds typically used to generate DTMs. The results of the tested algorithms will be discussed here based on the visual interpretation of the bare-earth point cloud and meshed points (2.5D Delaunay Triangulation at max 60m edge length). Meshing the ground points shows a sensitive reaction to remaining above-ground points which were not identified or misclassified by the respective algorithm.

Firstly the identification of the building present in the study area will be addressed. Out of the 5 methods only 3 successfully removed the rooftop in the ground class, Photoscan, LAStools and CSF. Hereby LAStools is the only software that classified the house as building (class value 6 - ASPRS 2011). CANUPO and the PMF left larger remainders of the rooftop in the bare-earth model (compare Fig. 21).

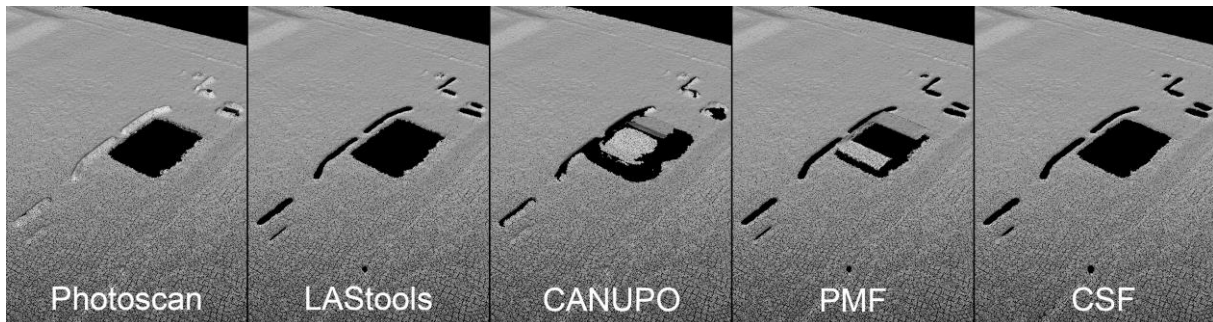


Fig. 21 Oblique close-up view of the building and parked cars of the Gail test site.

The class descriptor purely based on the dimensionality criterion as used by CANUPO hereby detects a rather 2D surface for both actual ground surface and the roof of the house. The rooftop cannot be filtered since sudden jumps in elevation are not considered by the classifier opposed to the 3 methods that effectively removed the building. In the case of the PMF a larger cell size did remove the roof of the building completely though leaving smaller vegetation such as the hedges close to the house and the planted young trees along the river bank.

All cars parked besides the building and on the larger gravel parking lot were only fully removed by CANUPO at 99% classification confidence, the PMF and the CSF. Photoscan misclassified all cars as ground while LAStools removed the car rooftops though leaving the sides which are clearly visible in the meshed cloud. The same applies to hedges and smaller

vegetation (see Fig. 21). Though classifying the tops as non-ground both LAStools and Photoscan fail remove these object entirely when only ground points are extracted. In both cases a smaller distance to ground threshold (ground offset) with for example 0.05m does avoid retaining the base of non-ground features in the bare-earth model. However this also causes a low confidence in the classification of points close to the ground and a class label 1 (unclassified) with LAStools and non-ground in Photoscan. If the extraction of ground points rather than the utilization of the fully classified cloud is the main purpose of the classification a small ground distance threshold is advisable. This should especially be considered with SfM derived point clouds based on UAS imagery where small surface variations potentially caused by very small herbivorous vegetation shall be removed.

The forested patches were removed identified and removed in the ground model by all algorithms but CANUPO. Again owing to a classifier being based purely on dimensionality of features portions of the forest canopy that appear rather planar are mistakenly as ground. Though increasing the classification confidence to 99% some of these patches are eliminated. Further filtering with by for example volume density thresholding or a statistical outlier filter can remove the remaining forest points from the bare-earth model though this was not the intention of the comparison.

The meshed ground surface displays the performance of the algorithms well and by close inspection it was determined that the overall most reliable bare-earth identification was achieved by the Cloth Simulation Filter. With its simple parameter setup and the overall shortest runtime the method can be applied to other scenes with minimal time spent on parameter tweaking giving it a definite advantage over the other methods that do often require lengthy setting adjustments.

In general it was shown that the tested algorithms can be applied to SfM derived point clouds though designed for use with LiDAR data. For classification into multiple classes LAStools offers functionality accurately determining between buildings and high vegetation in addition to ground detection. Applying CANUPO with several binary classifiers the cloud can be broken into finer classes also though the extensive manual work for training a classifier needs to be considered. Furthermore SfM point clouds do have limitations when using solely dimensionality as class descriptor. Recording only the surface without penetrating features results in two dimensional shapes for vegetation such as trees. Utilizing a true 3D cloud with points below the forest canopy as acquired by a LiDAR sensor has definite benefits to separate

various classes using CANUPO, especially with classifiers designed to distinguish between two vegetation types (e.g. trees and bushes).

For a rapid ground-only detection a SfM derived point cloud can also be classified in PhotoScan internally. The few parameters to be chosen and the short computational time offer the ability to find the most suitable setup for a scene rather quickly and the identification of low-noise is also beneficial.

Although parameters were chosen carefully for the PMF it did not result in optimal ground extraction keeping portions of some above-ground features. The inability to be applied to the point cloud by parallel computation on multiple cores resulted in a runtime far above other tested methods.

For the use in riverine monitoring and especially for studying riverine geomorphology LAStools provides the best performance in classification out of the proprietary software tested. Multiple class identification and the ability to fine-tune parameters to match a specific scene and scale is beneficial for monitoring river systems by point clouds in both the commercial and the scientific sector (see Fig. 22).

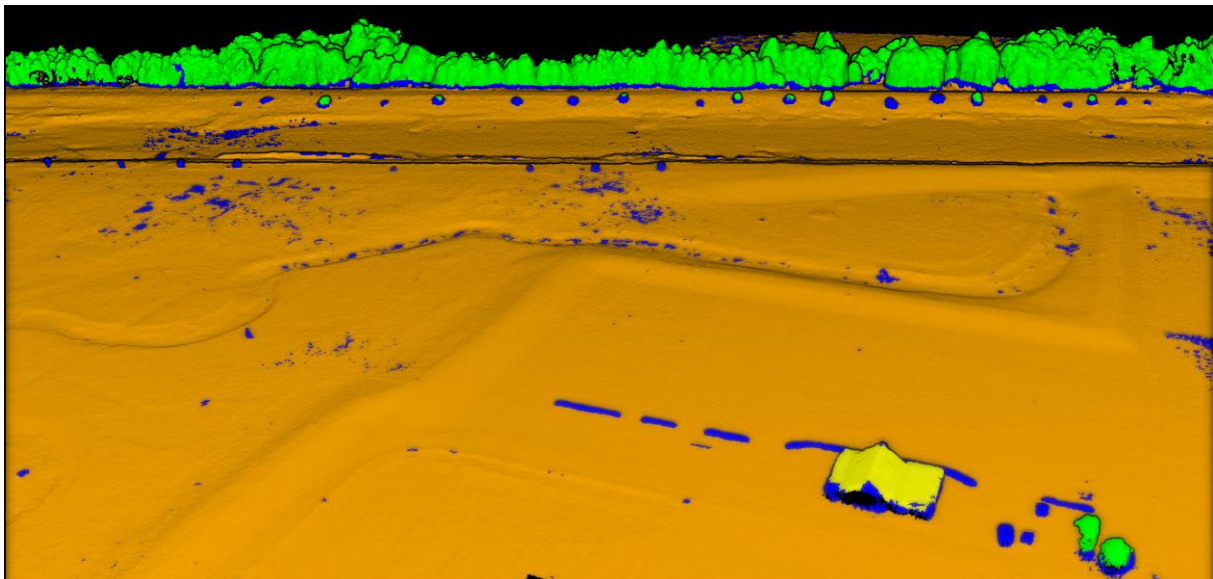


Fig. 22 View of the LAStools classification results in oblique perspective looking NE. Ground in brown, unclassified in blue, vegetation in green and buildings in yellow.

The recently developed CSF delivered the best performance out of the open-source algorithms though is limited when further classification of above ground features is required. When the division into finer classes by surface properties is required (e.g. grain sizes) CANUPO offers functionality particularly interesting for scientific work on smaller scale study areas.

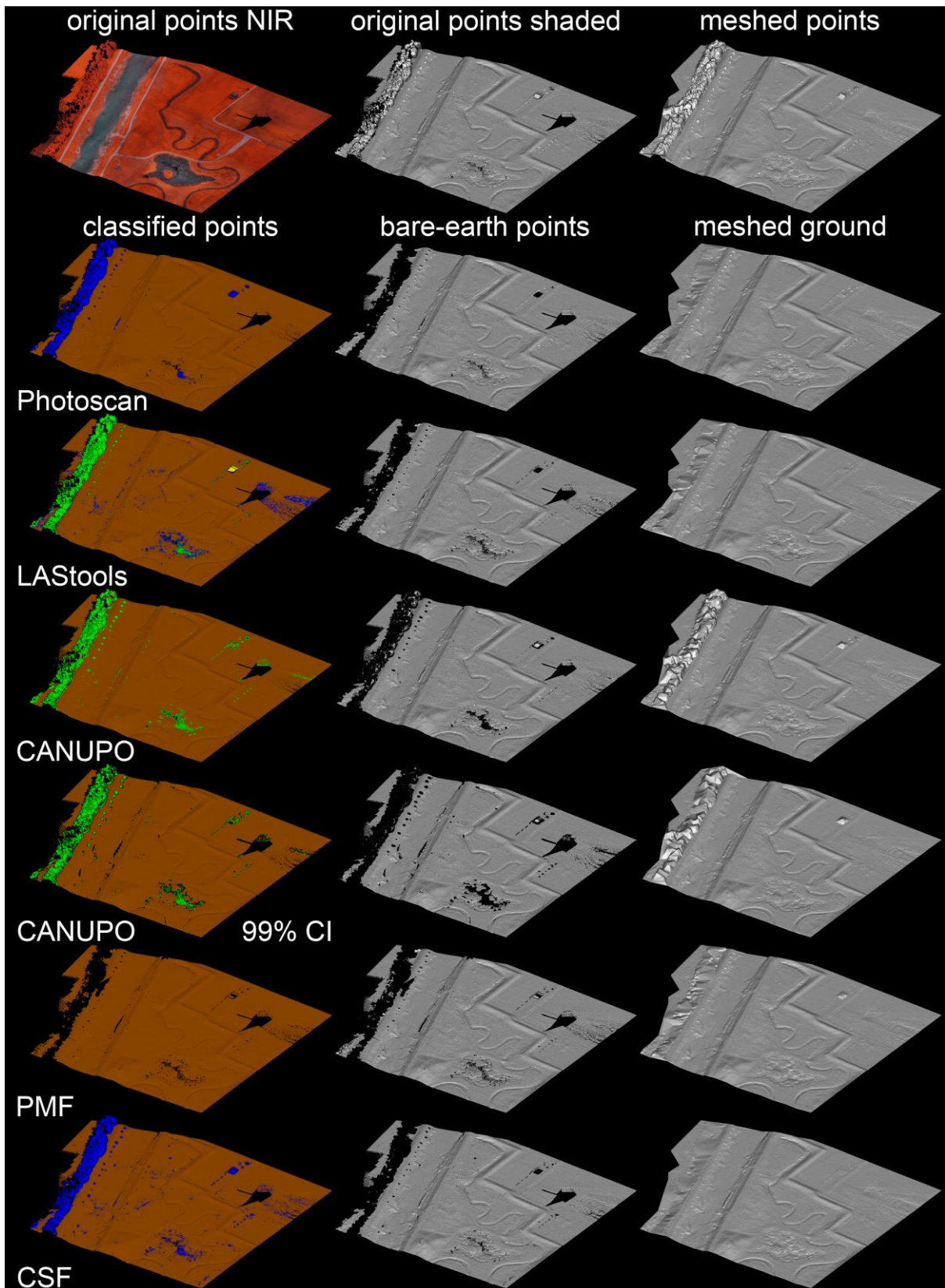
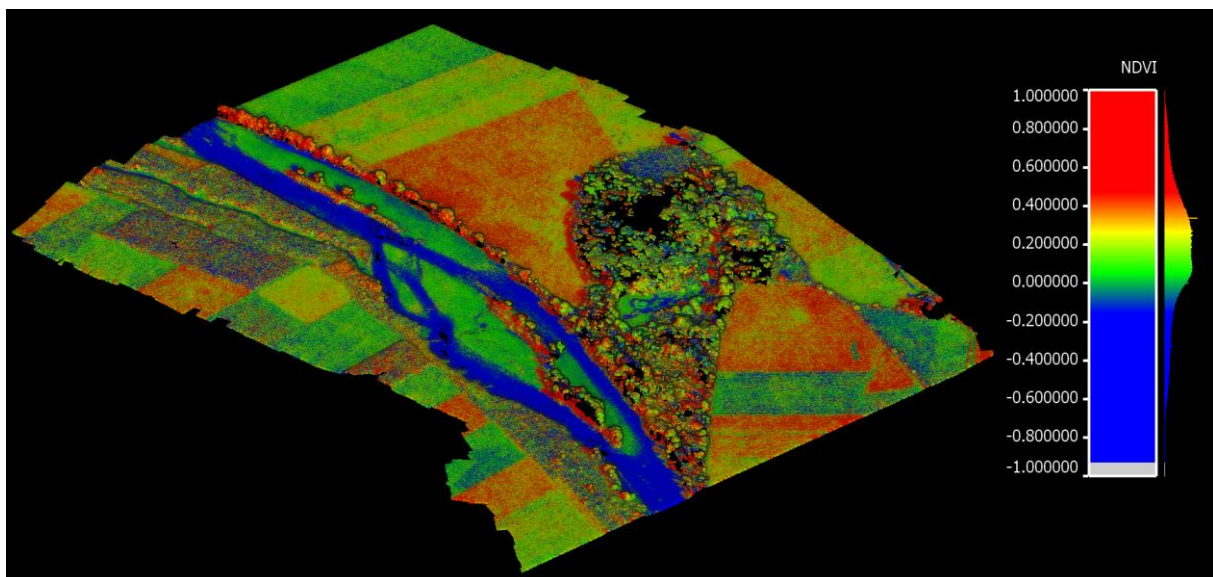


Fig. 23 Visual comparison of applied classification methods in oblique viewing angle. Scene computed from 02.10.2015 NIR Bramor mission flown in the Feistritz study area. The left column shows the classified point cloud with colorization for following classification labels: brown=ground, blue=unclassified, green=vegetation and yellow=buildings. The column in the center shows the extracted bare-earth points identified by respective algorithms. The right column depicts of a meshed version of the bare-earth clouds to better visualize remainders of non-ground points.

5.2 NDVI and NDWI Point Cloud

Having calculated the NDVI and the NDWI for the exemplary point cloud of the 12.10.2015 Bramor mission at the Drau study site results are presented in Fig. 24. Both indices are ranging from -1 to 1 with high positive values suggesting vegetation cover with high chlorophyll content for the NDVI and surfaces with high water content for the NDWI. Negative values on the other hand suggest an absence of vegetation and water. The river is clearly delineated by visual inspection by both NDVI and NDWI. While the NDVI shows the actual water surface of the Drau in its negative values the NDWI reveals water content on the sand banks within the channel too. Riparian vegetation such as the trees growing on the banks is shown as high positive values in the NDVI values. Clearly visible is also the stark contrast between the various agricultural fields surrounding the study area showing the reflective response of different crops and vegetational statuses. Areas affected by shadow at the edge of the forest deliver falsified NDVI and NDWI values as it is to be expected.

Generally these results may be viewed as proof-of-concept and conclusions about the actual status of features on ground based on these indices need to be drawn with great care. This is especially so since the reflectance information in the imagery is uncalibrated and affected by fast changing light situations due to the UAVs close proximity to the ground (Daniel McKinnon 2014). However with the possibility laid out to combine spectral indices and morphology information by directly calculating them on point clouds holds potential for future implications, also in direct relation to fluvial scientist striving to gain a holistic perspective on these dynamic systems.



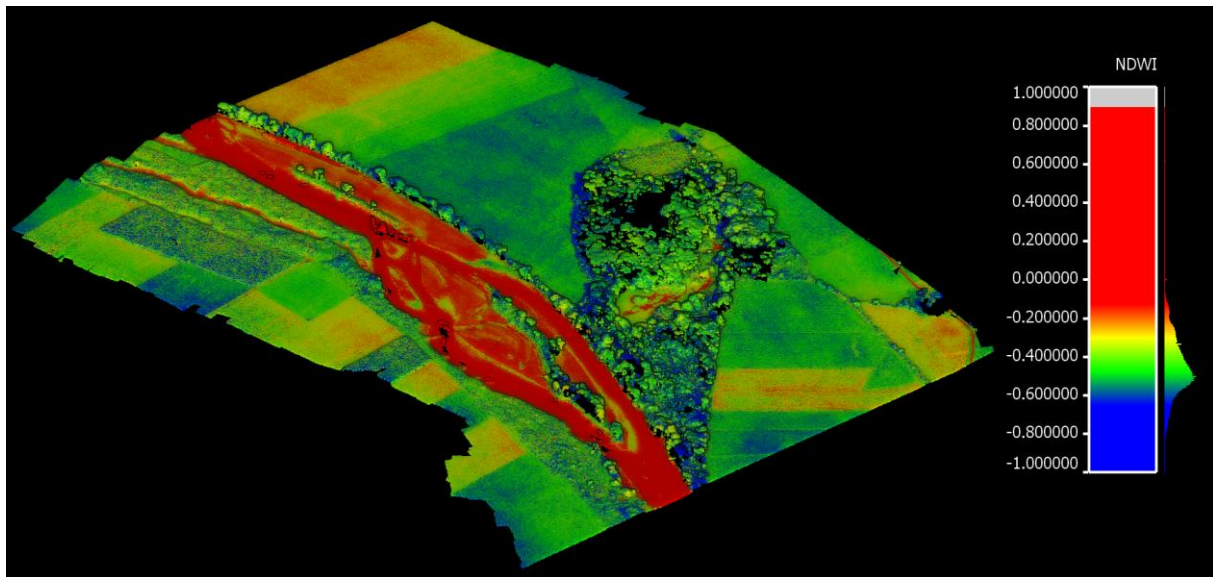


Fig. 24 NDVI and NDWI calculated on the 12.10.2015 Bramor mission in Obergottesfeld. Oblique view with color scale based on ± 1 SD around the mean. NDVI = mean 0.16 (SD 0.31), NDWI = mean -0.39 (SD 0.26).

5.3 Quantified Submerged Topography

For the exemplary dataset of the Gail study site (22.04.2015 RGB) the bottom topography and water depth was successfully derived with refraction correction applied. This was done for a section of the channel that is not influenced by shadows of trees and where the surface roughness of the water is relatively low (near to no white water). Results are visualized in Fig. 25 and show the continuous representation of the river bed in this section.

However noise points are observed where around the groynes at the northern bank of the river. Here the man-made structure has seemingly created altered hydraulic conditions that led to scour holes similar to sediment erosion behind bridge pillars. The water is much deeper in these parts and the texture of the river bed is clearly visible in the UAV imagery leading to noise points when the scene was reconstructed by the SfM approach. Since the reconstruction heavily relies on information within the image in the form of texture in the scene and contrast in the imagery the success of an SfM method for submerged topography estimations is water depth dependent (Woodget *et al.* 2015, Smith *et al.* 2016).

To further evaluate the representation of the submerged topography and the success of the refraction correction the SfM point cloud was held against the reference data acquired by echo sounding at cross sections in 2014. The location of the respective cross sections is shown in Fig. 28. Comparing the SfM obtained data to the sonar sampled points the general shape of the riverbed is well presented. Though some discrepancies can be observed, e.g. cross section #17 closest to the left river bank (Fig. 26) in which case it is not clear whether the SfM method

failed to reconstruct the steep gradient or the bed form has changed in the period between the data acquisition dates (4 months).

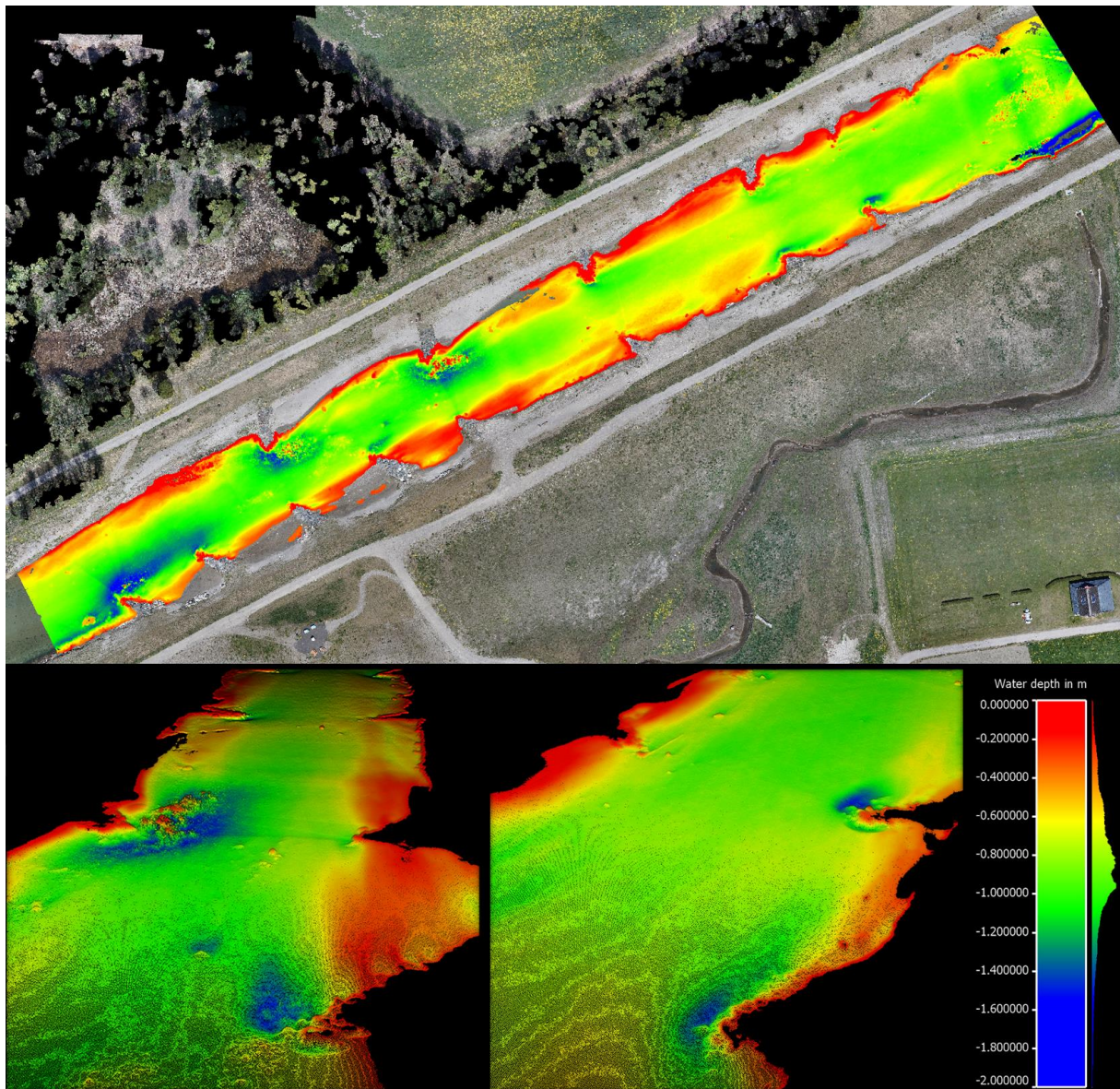


Fig. 25 Water depth with applied refraction factor mapped onto subset of the point cloud (04.22.2015 Bramor mission). Color scale based on 2SD around the mean. Water depth mean = -0.86m (SD 0.35m). Details given in oblique view with point shading.

The vertical root mean square error between the reference sonar data and SfM points extracted at the along these cross sections is 0.33m when not corrected for refraction and 0.19m with refraction correction applied. Although Woodget *et al.* 2015 reported a maximum error of 0.05m following the application of refraction correction it has to be kept in mind that the SfM point cloud in this case was manually aligned to the reference data (RMS = 0.2m), which in turn was referenced to the surveyed GCP locations (RMS = 0.24m). Furthermore it is known that errors in observations increase proportional to survey range (Smith *et al.* 2016).

The flight altitude of the UAV for the 2015 study of Woodget *et al.* was 30m at maximum while the RPAmSS was acquiring imagery from 100m AGL. Considering these factors and given the error of registration for absolute location and hence imperfect alignment with the echo sounding cross sections the positive effect of the refraction correction, as in a reduction of the root mean square error value, was still observed.

Further detailed examination of the cross sections supports this observation. Fig. 26 provides an example of three cross sections to visualize the influence of the refraction correction on the SfM point cloud. By applying the simple refractive factor of 1.34 the SfM data clearly matches the sonar measurements better which is reflected by the improvement in root mean square error as well.

Cross sections with areas of deeper water depth, like #17 where a pool was formed around the groynes, generally depict of higher errors with and without refraction correction. This fact is owing to the previously mentioned noise points that exist as a consequence of lacking texture in these deeper parts of the channel. These points were not picked up by the noise filtering process applied in this study since a more aggressive filtering method also removed valid points. Results show that the point cloud the workflow was tested on start to reveal noise at a water depth of 1.4m and below.

In general it was shown that a workflow similar to the method suggested by Woodget *et al.* was applicable to point cloud rather than raster data. Furthermore the extraction of the river boundary was extracted by a threshold filtering approach instead of simple manual point picking which decreases uncertainty and improves on replicability. The overall root mean square error observed for submerged topography was 0.19m following the correction of water refraction. The result for the 22.04.2015 dataset hence falls within the expected error range of 0.1-0.2m at a survey range of 100m (Smith *et al.* 2016).

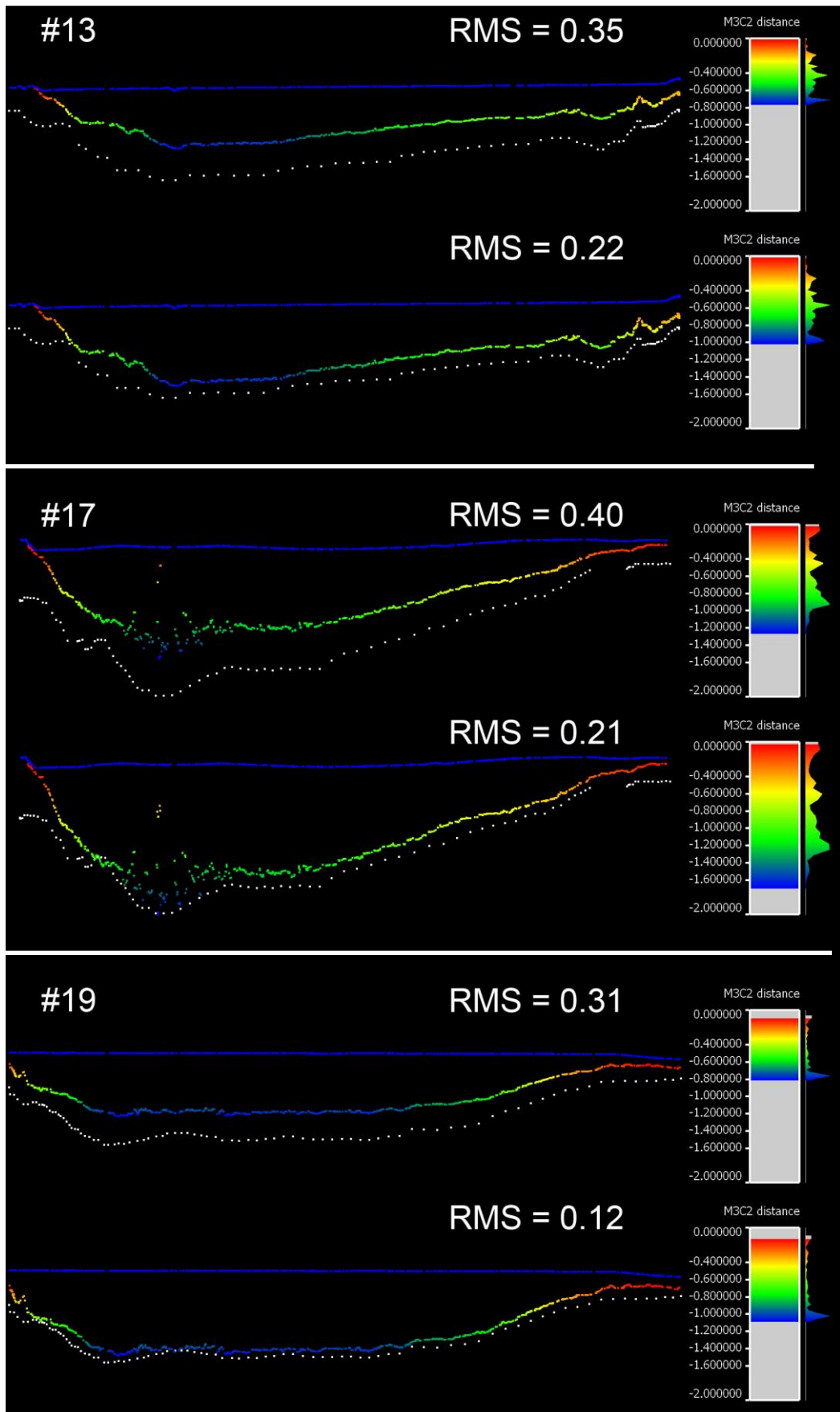


Fig. 26 Comparison of 2014 acquired sonar cross section (white, the simulated water surface (blue)) and SfM derived river bottom (water depth mapped onto points as color scale). Examples given for three cross sections with #17 affected by water depth related noise. Each example shown without (top) and with (bottom) refraction correction applied and their corresponding root mean square deviation from the sonar

6 Discussion

The assessment of UAS-SfM point clouds has demonstrated the ability to produce multi-temporal, spatially continuous datasets that can be utilized for classification, spectral index calculation and estimation of exposed as well as submerged topography in respect to monitoring dynamic river environments. In addition to the applied methods towards riverine analysis special attention was laid on preprocessing of SfM point clouds hence presenting a substantial part of the executed work. It was found that datasets of the two study sites depict of shifts in their absolute position making comparison between the multi-temporal point clouds and to reference data infeasible. Fine alignment for absolute referencing was undertaken though introducing a lengthy manual registration procedure. Furthermore the high data volumes owing to the high point densities achieved by a SfM-MVS approach stated computational challenges. An appropriate sub-sampling method to reduce file size as well as to normalize point densities (min. distance horizontal = 10cm, vertical = 5cm) was established and applied to all datasets. The developed procedure enabled further processing of the data at the full extent of the study sites on a standard PC (i7 3.4Ghz, 8Gb RAM) without compromising the representation of general feature geometry. In case more computational power is available and higher point densities are requested a spatial sub-sampling approach is still recommended when neighborhood dependent algorithms are to be applied at later processing stage. As a part of the preprocessing workflow the sub-sampled point clouds were filtered to identify noise which can cause false classification and introduce bias to analysis results. With the proposed three-stage filter observed noise was successfully filtered to a great extent, in particular sub-surface low noise. However some noise remained, specifically in water covered areas where image matching was restricted due to low texture. While a more “aggressive” filter was considered the execution on all acquired point clouds led to the identification of valid points as noise. This is due to the variable degrees of noise present throughout acquisition dates owing to variation in illumination, water turbidity and foliage which affect the illustration of texture in the imagery – the key factor for successful reconstruction of scenes by SfM-MVS. The number of complicating factors in SfM-photogrammetry that determine model quality and the linked compromised reproducibility in successive surveys in fact is perhaps the biggest weakness of such approach.

The observed inconsistencies in absolute location, completeness (e.g. gaps in model due to forest cover, turbid water) and noise levels amongst the point clouds demonstrate that a large

number of quality thresholds must be determined in order to implement SfM point clouds as monitoring tool. Hereby understanding the theory behind the SfM based reconstruction and associated influential factors is crucial to reduce data related uncertainty and extensive preprocessing. Carrivick *et al.* 2016 suggest to “get under the bonnet” of SfM-MVS to become a more critical end user.

The planned classification was conducted on the preprocessed point clouds testing five different algorithms. Three of the examined methods are primarily developed to identify ground point to create bare-earth model, separating the cloud ground and non-ground features. The only exception is the commercial software LAStools allowing the automatic detection of buildings, vegetation and ground. The CANUPO plugin of CloudCompare offers a different functionality than the other algorithms in a sense that the method is used to separate the cloud in user defined binary classes. An objective comparison between all algorithms revealed strengths and weaknesses of the methods for their use with SfM point clouds. The Progressive Morphological Filter did not show desirable results requiring tedious parameter setup, extracting only ground points, deleting their color information and by far exceeding the run-time of the other algorithms (32h versus several minutes). PhotoScans built in classification module can deliver fast classification of ground and non-ground features though did not reliably remove small non-ground features (e.g. hedges, see Fig. 21 Oblique close-up view of the building and parked cars of the Gail test site. Although offering the creation and the classification of point clouds in a single software package it was found that the few available parameters limit fine tuning of the algorithm. Better adjustability and performance is offered by LAStools making it the overall most advanced classification method. Alternatively the recently released open-source Cloth Simulation Filter delivered accurate distinction between ground and non-ground points. With few comprehensible parameters and the shortest computational time out of the tested methods the CSF is a valuable new tool, especially for the fast generation of bare-earth models of large datasets.

In contrast to LiDAR SfM point clouds describe the “visible” surface of features and cannot penetrate vegetation. The success of dimensionality reliant CANUPO classification method is hence limited due to the lack of points within the volume of vegetation. As it was expected forest canopy was hence classified as ground where relatively planar regions were detected. The general concept of allowing the user to define and train classifiers with CANUPO however is unique. It is believed that the method holds great potential for the classification of SfM point

clouds given further development such as the extension of criteria used as descriptor. Here the inclusion of color information would truly be beneficial to enable a hybrid geometrical-spectral distinction of features given that a SfM-MVS approach produces colored point clouds in any case.

The possibility of calculating spectral indices directly on point clouds was also evaluated as part of this study. On the basis of the RGB and NIR information acquired in consecutive RPAmSS flights it was tested whether the three dimensional derivation of the Normalized Differenced Vegetation Index and the Normalized Difference Water Index is feasible. It was shown that the spectral information of the RGB and NIR point cloud can successfully be merged into a single multispectral one by assigning color values based on shortest point-to-point distance. The derived indices indicate possible application scenarios in riverine studies where point clouds provide more detailed information than typical 2D grid data, e.g. NDVI based identification of vegetation in steep river banks. However the initial results presented were not further investigated due to lacking calibration of the reflectance values and reference data for validation purposes. Further investigation in the concept and influencing factors such as the fast changing illumination constituent to UAV based data capture is needed. Still general feasibility of multispectral point clouds and derived spectral indices was demonstrated may give fluvial scientist a new tool to holistically assess river environments.

Finally it was shown that bathymetric estimations can be undertaken on the basis of SfM point clouds. By applying the refractive index for clear water submerged topography was derived at a root mean square error of 0.19m for a test dataset of the Gail study site. Woodget *et al.* claim to be the first to have evaluated SfM derived data for quantification of submerged fluvial topography. Although their observed maximum error following refraction correction is lower there are some key differences between their and the current study. Their survey range was 30m compared to our image acquisition at 100m AGL. Furthermore their study site presented a maximum water depth of 0.7m while the examined Gail channel depicts of water depths as low as 2m and noise present at 1.4 and below. While they used DSM raster for processing it was shown here that point clouds may act as data source also. In this respect point clouds are the preferable format as they are the primary output of the SfM method and gridding inevitably introduces uncertainty especially in steep terrain.

The method to correct for refraction general relies a modelled water surface to calculate water depth. Here the manual extraction of elevations along the edge of the water as

undertaken by Woodget *et al.* was improved on by a RGB and density thresholding approach which delivered continuous data points along the water boundary. It is believed that the utilization of the Normalized Difference Water Index further improves and simplifies the extraction of the water boundary. However in the case of the test dataset used no NIR mission was flown.

Albeit the described workflow performed well on the exemplary data further testing is required to evaluate the applicability of SfM based bathymetry estimations for riverine monitoring. While the Gail depicted of very clear water conditions with little to no surface roughness on the present acquisition date 22.04.2105 further studies investigating the replicability of the method at various turbidity levels and different study sites are needed to draw further conclusions. Though it is clear that impediment in deriving accurate three dimensional data by SfM will always exist when matching image features that contain turbid water, ripples, reflection and shadow.

The overall results of the study illustrate the potential of the described workflows to extract valuable information for fluvial science and management. The capabilities of SfM point clouds to significantly increase topographic detail over traditional field sampling methods offers great research opportunities. Given adequate familiarization with influential factors in data acquisition by UAS as well as in data processing by SfM the approach facilitates an increase in extent and frequency of riverine surveys, enabling better understanding of these dynamic environments. Furthermore it was shown that SfM point clouds can be used for remote sensing techniques applied in fluvial studies where typically raster data are utilized as basis for calculation, e.g. NDWI derivation and bathymetric estimations. Although outputs of SfM-photogrammetry and derived products can be visually stunning they are by no means error free. As users of this technology we need to understand potential sources of these errors. This is especially true considering the increasingly affordable UAS technology making the reconstruction of scenes with user-friendly SfM software available to almost anyone. As scientists however we need to comprehend all parameters that may affect results and avoiding to see SfM-photogrammetry as “black-box” approach.

7 Future Work

The study has outlined and evaluated several methods for the utilization of SfM point clouds to monitor river environments. Using UAS for SfM-photogrammetry as a tool to holistically

study dynamic fluvial systems and to cut down on tedious field work is still at an early stage of development although potential future applications are plentiful. A key area that would benefit from further research is concerning the acquisition of the data. Specifically aiming towards avoidance of geometric errors and improvement of positional accuracy further investigation is needed. Here the effects of convergent versus typical parallel flight lines (oblique imagery) as suggested by James and Robson 2014 and Smith *et al.* 2016 should be targeted to quantify differences in reconstructed detail and respective accuracy. Furthermore the number of essential GCPs and their layout for study areas with variable topography to achieve a certain desired accuracy should be targeted. These factors are especially important for repeated surveys when changes in morphology are to be addressed.

In terms of the classification of SfM point clouds there is potential for development considering that current classification algorithms are primarily designed for LiDAR data hence only relying on geometric properties. Exploiting the color information stored on SfM point clouds in conjunction with existing geometric classification approaches could yield higher levels of class discrimination and corresponding accuracy. A proposal for such method is the combination of the open-source Cloth Simulation Filter for fast and reliable ground detection and multiple stage CANUPO classification of remaining non-ground features for finer class separation. Here the inclusion of color values as further descriptor would truly be beneficial. Such extension of the CANUPO classifier was already proposed by Daniel Girardeau-Montaut, the main developer of CloudCompare in 2015 (<https://youtu.be/XF41Qj4zaVg>), but has yet to be implemented. A hybrid classification approach with CSF and CANUPO offers great flexibility especially for specific analyses where detailed training of the classifier at user defined scales is needed. An example for riverine monitoring is the automatic detection of driftwood within the channel (Fig. 27) and future application areas could go as far as grainsize estimations

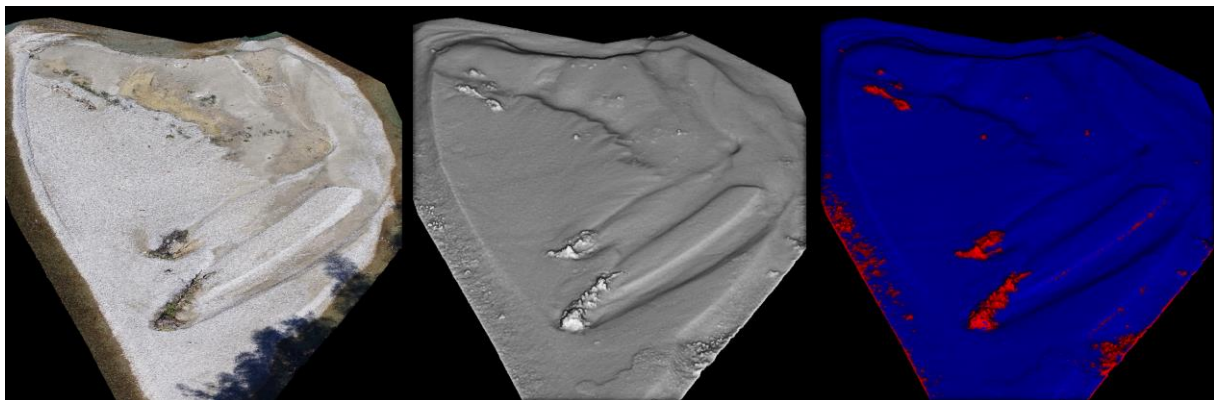


Fig. 27 Deadwood identification on a sandbank of the Drau study site. Binary classification of deadwood (red) vs. everything else (blue) by CANUPO classifier (trained on two scales: 0,5m and 1m).

combining several binary classifiers in CANUPO. However such specific areas of application currently still involve a great deal of manual segmentation, testing and evaluation of results. Another scope of application that requires more research is the quantification of submerged topography by means of SfM point clouds. While the fundamental method for the extraction of the water boundary and the refraction correction was illustrated further improvement may stem from the utilization of multispectral information. Another area of investigation specifically towards bathymetric estimations is the use of a polarization filter in front of the camera lens. Such filter might be able to suppress glare and reflection by filtering scattered unorganized light (Matsuyama *et al.* 2004) and hence increasing the pictured underwater texture.

Overall there are numerous research areas that indicate that the full capabilities of SfM-MVS point clouds have yet to be realized (Smith *et al.* 2016). However with further technological advances in sensor design and unmanned platforms for data capture as well as the ongoing progress in image matching algorithms SfM point cloud specific analyses have the potential to be a powerful, low-cost addition to the fluvial remote sensing toolkit (Dietrich 2016).

8 References

- Abellán, A., *et al.*, 2009. Detection of millimetric deformation using a terrestrial laser scanner: Experiment and application to a rockfall event. *Natural Hazards and Earth System Science*, 9 (2), 365–372.
- Abellán, A., Vilaplana, J.M., and Martínez, J., 2006. Application of a long-range Terrestrial Laser Scanner to a detailed rockfall study at Vall de Núria (Eastern Pyrenees, Spain). *Engineering Geology*, 88 (3–4), 136–148.
- Agisoft. *PhotoScan* [online]. Available from: www.agisoft.com [Accessed 29 May 2016].
- Alcantarilla, Nuevo, and Bartoli, 2013. Fast Explicit Diffusion for Accelerated Features in Nonlinear Scale Spaces. In: *British Machine Vision Conf. (BMVC)*.
- Antonarakis, A.S., *et al.*, 2010. Determining leaf area index and leafy tree roughness using terrestrial laser scanning. *Water Resources Research* [online], 46 (6). Available from: <http://onlinelibrary.wiley.com/doi/10.1029/2009WR008318/full>.
- APOS. *Austrian Positioning Service* [online]. Available from: http://www.bev.gv.at/portal/page?_pageid=713,1571538&_dad=portal&_schema=PORTAL [Accessed 26 Jun 2016].
- Arneson, J., 2015. Riparian Area Vegetation Response to High and Low Flows in the Platte River Through Digital Imagery.
- Arnó, J., *et al.* Leaf area index estimation in vineyards using a ground-based LiDAR scanner. *Precision Agriculture* [online], 14 (3), 290–306. Available from: <http://link.springer.com/article/10.1007/s11119-012-9295-0/fulltext.html>.
- ASPRS, 2011. *LAS Specification: Version 1.4 – R6* [online], The American Society for Photogrammetry & Remote Sensing. Available from: http://www.asprs.org/wp-content/uploads/2010/12/LAS_1-4_R6.pdf.
- Axelsson, P., 2000. DEM generation from laser scanner data using adaptive TIN models.
- Bailly, J.-S., *et al.*, 2010. Geostatistical estimations of bathymetric LiDAR errors on rivers. *Earth Surface Processes and Landforms*, 35 (10), 1199–1210.
- Barnea, S., Filin, S., and Alchanatis, V., 2007. A supervised approach for object extraction from terrestrial laser point clouds demonstrated on trees. *International Archives of the Photogrammetry, Remote Sensing and Spatial Information Sciences*, 36.
- BMLFUW, 2011. *LIFE Obere Drau II* [online]. Available from: http://www.life-drau.at/?page=Allgemeines&id=5&menu=7&lng=1&sub_id=3 [Accessed 14 Feb 2016].
- BMLFUW, 2014. *LIFE Gail* [online]. Available from: <http://www.life-gail.at/?tpl=text&id=72> [Accessed 14 Feb 2016].
- Brasington, J., Vericat, D., and Rychkov, I., 2012. Modeling river bed morphology, roughness, and surface sedimentology using high resolution terrestrial laser scanning. *Water Resources Research* [online], 48 (11). Available from: <http://onlinelibrary.wiley.com/doi/10.1029/2012WR012223/full>.
- Brodu, N. and Lague, D., 2012. 3D point cloud classification of complex natural scenes using a multi-scale dimensionality criterion: applications in geomorphology. *Geophysical Research Abstracts*, 14, EGU2012-4368.
- Carbonneau, P.E. and Piégay, H., 2012. *Fluvial Remote Sensing for Science and Management*. Chichester, UK: John Wiley & Sons, Ltd.
- Carrivick, J.L., Smith, M.W., and Quincey, D.J., 2016. *Structure from Motion in the Geosciences*: Wiley.
- Changchang Wu. *VisualSFM* [online]. Available from: ccwu.me/vsfm [Accessed 25 Aug 2016].
- Dandois, J.P. and Ellis, E.C., 2013. High spatial resolution three-dimensional mapping of vegetation spectral dynamics using computer vision. *Remote Sensing of Environment*, 136, 259–276.
- Daniel McKinnon, 2014. *Misconceptions about UAV-collected NDVI imagery and the Agribotix experience in ground truthing these images for agriculture* [online]. Available from: <http://agribotix.com/blog/2014/6/10/misconceptions-about-uav-collected-ndvi-imagery-and-the-agribotix-experience-in-ground-truthing-these-images-for-agriculture/> [Accessed 28 Aug 2016].

- Darby, S.E., 1999. Effect of Riparian Vegetation on Flow Resistance and Flood Potential. *Journal of Hydraulic Engineering*, 125 (5), 443–454.
- Dietrich, J.T., 2016. Riverscape mapping with helicopter-based Structure-from-Motion photogrammetry. *Geomorphology*, 252, 144–157.
- Evans, J.S. and Hudak, A.T., 2007. A multiscale curvature algorithm for classifying discrete return LiDAR in forested environments. *IEEE Transactions on Geoscience and Remote Sensing* [online], 45 (4), 1029–1038. Available from: <http://treesearch.fs.fed.us/pubs/download/29032.pdf>.
- Fausch, K.D., *et al.*, 2002. Landscapes to Riverscapes: Bridging the Gap between Research and Conservation of Stream Fishes A Continuous View of the River is Needed to Understand How Processes Interacting among Scales Set the Context for Stream Fishes and Their Habitat. *BioScience* [online], 52 (6), 483–498. Available from: <http://bioscience.oxfordjournals.org/content/52/6/483.full>.
- Fischler, M.A. and Bolles, R.C., 1981. Random sample consensus: A paradigm for model fitting with applications to image analysis and automated cartography. *Communications of the ACM*, 24 (6), 381–395.
- Fonstad, M.A., *et al.*, 2013a. Topographic structure from motion: a new development in photogrammetric measurement. *Earth Surface Processes and Landforms*, 38.
- Fonstad, M.A., *et al.*, 2013b. Topographic structure from motion: a new development in photogrammetric measurement. *Earth Surface Processes and Landforms* [online], 38 (4), 421–430. Available from: <http://onlinelibrary.wiley.com/doi/10.1002/esp.3366/full>.
- Gehrke, S., *et al.*, 2010. Semi-global matching: An alternative to LIDAR for DSM generation. In: *Proceedings of the 2010 Canadian Geomatics Conference and Symposium of Commission I*.
- Gippel, C.J., 1995. Environmental Hydraulics of Large Woody Debris in Streams and Rivers. *Journal of Environmental Engineering*, 121 (5), 388–395.
- Grims, M., *et al.*, 2014. Low-cost Terrestrial Photogrammetry as a Tool for a Sample-Based Assessment of Soil Roughness. *Photogrammetrie - Fernerkundung - Geoinformation*, 2014 (5), 313–323.
- Heritage, G.L. and Milan, D.J., 2009. Terrestrial Laser Scanning of grain roughness in a gravel-bed river. *Geomorphology*, 113 (1-2), 4–11.
- Hodge, R., Brasington, J., and Richards, K., 2009a. Analysing laser-scanned digital terrain models of gravel bed surfaces: Linking morphology to sediment transport processes and hydraulics. *Sedimentology*, 56 (7), 2024–2043.
- Hodge, R., Brasington, J., and Richards, K., 2009b. In situ characterization of grain-scale fluvial morphology using Terrestrial Laser Scanning. *Earth Surface Processes and Landforms*.
- Hodge, R.A., 2010. Using simulated Terrestrial Laser Scanning to analyse errors in high-resolution scan data of irregular surfaces. *ISPRS Journal of Photogrammetry and Remote Sensing*, 65 (2), 227–240.
- Huang, J. and You, S., 2013. *Detecting Objects in Scene Point Cloud: A Combinational Approach*: IEEE. Available from: <http://ieeexplore.ieee.org/iel7/6598368/6599039/06599074.pdf?arnumber=6599074>.
- Jaboyedoff, M., *et al.* Use of LIDAR in landslide investigations: a review. *Natural Hazards* [online], 61 (1), 5–28. Available from: <http://link.springer.com/article/10.1007/s11069-010-9634-2/fulltext.html>.
- James, M.R. and Robson, S., 2014. Mitigating systematic error in topographic models derived from UAV and ground-based image networks. *Earth Surface Processes and Landforms*, 39.
- Javernick, L., Brasington, J., and Caruso, B., 2014. Modeling the topography of shallow braided rivers using Structure-from-Motion photogrammetry. *Geomorphology*, 213, 166–182.
- Kinzel, P.J., Legleiter, C.J., and Nelson, J.M., 2013. Mapping River Bathymetry With a Small Footprint Green LiDAR: Applications and Challenges 1. *JAWRA Journal of the American Water Resources Association*, 49 (1), 183–204.
- Kraus, K., 2007. *Photogrammetry: Geometry from images and laser scans*. 2nd ed. Berlin, New York: Walter De Gruyter.
- Kraus, K. and Pfeifer, N., 2001. Advanced DTM generation from LIDAR data. *International Archives Of Photogrammetry Remote Sensing And Spatial Information Sciences*, 34 (3/W4), 23–30.

- Lague, D., 2014. *What's the Point of a Raster? Advantages of 3D Point Cloud Processing over Raster Based Methods for Accurate Geomorphic Analysis of High Resolution Topography*.
- Lague, D., 2016. Full Waveform topo-bathymetric Airborne LiDAR [online]. Available from: https://geosciences.univ-rennes1.fr/IMG/pdf/Poster_lidar_topo_bathy_LAGUE.pdf [Accessed 29 Aug 2016].
- Lague, D., Brodu, N., and Leroux, J., 2013. *Accurate 3D comparison of complex topography with terrestrial laser scanner: application to the Rangitikei canyon (N-Z)*.
- Lane, E.W., 1954. *The Importance of Fluvial Morphology in Hydraulic Engineering*: U.S. Department of the Interior, Bureau of Reclamation, Commissioner's Office.
- Legleiter, C.J., 2012. Remote measurement of river morphology via fusion of LiDAR topography and spectrally based bathymetry. *Earth Surface Processes and Landforms*, 37 (5), 499–518.
- Legleiter, C.J., 2014a. A geostatistical framework for quantifying the reach-scale spatial structure of river morphology: 1. Variogram models, related metrics, and relation to channel form. *Geomorphology*, 205, 65–84.
- Legleiter, C.J., 2014b. A geostatistical framework for quantifying the reach-scale spatial structure of river morphology: 2. Application to restored and natural channels. *Geomorphology*, 205, 85–101.
- Legleiter, C.J., Roberts, D.A., and Lawrence, R.L., 2009. Spectrally based remote sensing of river bathymetry. *Earth Surface Processes and Landforms*, 34 (8), 1039–1059.
- Lejot, J., *et al.*, 2007. Very high spatial resolution imagery for channel bathymetry and topography from an unmanned mapping controlled platform. *Earth Surface Processes and Landforms*, 32 (11), 1705–1725.
- Longuet-Higgins, H.C., 1981. A computer algorithm for reconstructing a scene from two projections, 293 (5828), 133–135.
- Lowe, D.G., 2014. Distinctive Image Features from Scale-Invariant Keypoints. *International Journal of Computer Vision* [online], 60 (2), 91–110. Available from: <http://link.springer.com/content/pdf/10.1023%2FB%3AVISI.0000029664.99615.94.pdf>.
- Maltezos, E. and Ioannidis, C., 2015. Automatic detection of building points from LiDAR and dense image matching point clouds. *ISPRS Annals of Photogrammetry, Remote Sensing and Spatial Information Sciences*, II-3/W5, 33–40.
- Marc Pierrot Deseilligny. *MicMac* [online], IGN/ENSG. Available from: <http://logiciels.ign.fr/?Micmac> [Accessed 29 May 2016].
- Martin Isenburg. *math behind lasground* [online]. Available from: <https://groups.google.com/forum/#!topic/lastools/vgEKeV4peVo> [Accessed 25 Jul 2016].
- Marzahn, P., Rieke-Zapp, D., and Ludwig, R., 2010. *Statistical assessment of soil surface roughness for environmental applications using photogrammetric imaging techniques*.
- Matsuyama, T., Ishiyama, T., and Omura, Y., 2004. Nikon projection lens update. *In*: B.W. Smith, ed. *Microlithography 2004*: SPIE, 730.
- Mc Feeters, S.K., 1996. The use of the Normalized Difference Water Index (NDWI) in the delineation of open water features. *International Journal of Remote Sensing*, 17 (7), 1425–1432.
- Milan, D.J., Heritage, G.L., and Hetherington, D., 2007. Application of a 3D laser scanner in the assessment of erosion and deposition volumes and channel change in a proglacial river. *Earth Surface Processes and Landforms*, 32 (11), 1657–1674.
- Moskal, L.M., *et al.*, 2009. Lidar applications in precision forestry. *Proceedings of Silvilaser*, 154–163.
- Nagihara, S., Mulligan, K.R., and Xiong, W., 2004. Use of a three-dimensional laser scanner to digitally capture the topography of sand dunes in high spatial resolution. *Earth Surface Processes and Landforms*, 29 (3), 391–398.
- Noah Snively. *Bundler* [online]. Available from: <http://www.cs.cornell.edu/~snively/bundler>.
- Olsen, M.J., *et al.*, 2010. Terrestrial Laser Scanning-Based Structural Damage Assessment. *Journal of Computing in Civil Engineering*, 24 (3), 264–272.

- O'Neal, M.A. and Pizzuto, J.E., 2011. The rates and spatial patterns of annual riverbank erosion revealed through terrestrial laser-scanner surveys of the South River, Virginia. *Earth Surface Processes and Landforms*, 36 (5), 695–701.
- Otepka, J., *et al.*, 2013. Georeferenced Point Clouds: A Survey of Features and Point Cloud Management. *ISPRS International Journal of Geo-Information*, 2 (4), 1038–1065.
- Pix4D SA. *Pix4D* [online]. Available from: www.pix4d.com [Accessed 25 Aug 2016].
- Pool, G.C., 2002. Fluvial landscape ecology: Addressing uniqueness within the river discontinuum. *Freshwater Biology*, 47 (4), 641–660.
- Roman Hiestand. *Regard 3D* [online]. Available from: www.regard3d.org.
- Rosser, N.J., *et al.*, 2005. Terrestrial laser scanning for monitoring the process of hard rock coastal cliff erosion. *Quarterly Journal of Engineering Geology and Hydrogeology*, 38 (4), 363–375.
- Rothermel Mathias, K.W. *SURE* [online], Uni Stuttgart - Institut für Photogrammetrie. Available from: <http://www.ifp.uni-stuttgart.de/publications/software/sure/index.en.html> [Accessed 25 Aug 2016].
- Rouse, J.W., *et al.*, 1974. Monitoring Vegetation Systems in the Great Plains with ERTS. *NASA Special Publication*, 351, 309.
- RPAmSS | Remotely Piloted Aircraft Multi Sensor System* [online]. Available from: http://rpmss.cuas.at/rpamss/?page_id=43 [Accessed 13 Feb 2016].
- Schnabel, R., Wahl, R., and Klein, R., 2007. Efficient RANSAC for Point-Cloud Shape Detection. *Computer Graphics Forum* [online], 26 (2), 214–226. Available from: <http://cg.cs.uni-bonn.de/aigaion2root/attachments/schnabel-2007-efficient.pdf>.
- Schürch, P., *et al.*, 2011. Detection of surface change in complex topography using terrestrial laser scanning: Application to the Illgraben debris-flow channel. *Earth Surface Processes and Landforms*, 36 (14), 1847–1859.
- Serna, A. and Marcotegui, B., 2014. Detection, segmentation and classification of 3D urban objects using mathematical morphology and supervised learning. *ISPRS Journal of Photogrammetry and Remote Sensing*, 93, 243–255.
- Smith, M.W., Carrivick, J.L., and Quincey, D.J., 2016. Structure from motion photogrammetry in physical geography. *Progress in Physical Geography* [online], 40 (2), 247–275. Available from: <http://ppg.sagepub.com/content/40/2/247.full.pdf>.
- Smith, M.W. and Vericat, D., 2014. Evaluating shallow-water bathymetry from through-water terrestrial laser scanning under a range of hydraulic and physical water quality conditions. *River Research and Applications*, 30 (7), 905–924.
- Teza, G., *et al.*, 2008. Characterization of landslide ground surface kinematics from terrestrial laser scanning and strain field computation. *Geomorphology*, 97 (3-4), 424–437.
- The first generation of 2D hyperspectral camera is airborne* [online]. Available from: <http://www.rikola.fi/hyperspectralcamera.pdf> [Accessed 13 Feb 2016].
- Uddin, W., 2002. Evaluation of airborne LiDAR digital terrain mapping for highway corridor planning and design. *In: Proc. Pecora*, 10–15.
- Ullman, S., 1979. The Interpretation of Structure from Motion. *Proceedings of the Royal Society B: Biological Sciences*, 203 (1153), 405–426.
- Wallace, L., *et al.*, 2012. Development of a UAV-LiDAR System with Application to Forest Inventory. *Remote Sensing* [online], 4 (6), 1519–1543. Available from: <http://www.mdpi.com/2072-4292/4/6/1519/pdf>.
- Wallace, L., Lucieer, A., and Watson, C.S., 2014. Evaluating Tree Detection and Segmentation Routines on Very High Resolution UAV LiDAR Data. *IEEE Transactions on Geoscience and Remote Sensing*, 52 (12), 7619–7628.
- Wang, Z.Y., Lee, J., and Melching, C.S., 2014. *River Dynamics and Integrated River Management*: Springer Berlin Heidelberg.
- Watson, G.A., 2006. Computing Helmert transformations. *Journal of Computational and Applied Mathematics*, 197 (2), 387–394.

- Watts, A.C., Ambrosia, V.G., and Hinkley, E.A., 2012. Unmanned aircraft systems in remote sensing and scientific research: Classification and considerations of use. *Remote Sensing*, 4 (6), 1671–1692.
- Westaway, R.M., Lane, S.N., and Hicks, D.M., 2001. Remote sensing of clear-water, shallow, gravel-bed rivers using digital photogrammetry. *Photogrammetric Engineering and Remote Sensing*, 67 (11), 1271–1282.
- Wiens, J.A., 2002. Riverine landscapes: Taking landscape ecology into the water. *Freshwater Biology*, 47 (4), 501–515.
- Woodget, A.S., et al., 2015. Quantifying submerged fluvial topography using hyperspatial resolution UAS imagery and structure from motion photogrammetry. *Earth Surface Processes and Landforms*, 40 (1), 47–64.
- Zander, L.-L., 2015. *Environmental Monitoring and Change Detection of Dynamic River Environments regarding Vegetation and Geomorphology*. Master thesis. Carinthia University of Applied Sciences.
- Zhang, K., et al., 2003. A progressive morphological filter for removing nonground measurements from airborne LIDAR data. *IEEE Transactions on Geoscience and Remote Sensing*, 41 (4), 872–882.
- Zhang, W., et al., 2016. An Easy-to-Use Airborne LiDAR Data Filtering Method Based on Cloth Simulation. *Remote Sensing*, 8 (6), 501.
- Zhang, Y., et al., 2015. *Rape plant NDVI 3D distribution based on structure from motion*, 31 (17).
- Zhou, G., et al., 2009. Foreword to the Special Issue on Unmanned Airborne Vehicle (UAV) Sensing Systems for Earth Observations. *Geoscience and Remote Sensing, IEEE Transactions on* [online], 47 (3), 687–689. Available from: <http://ieeexplore.ieee.org/iel5/36/4786573/04786580.pdf?arnumber=4786580>.

Annex



Fig. 28 Location of echo sounding samples acquired at cross sections of the Gail on the 09.12.2015 at approx. 20m intervals.

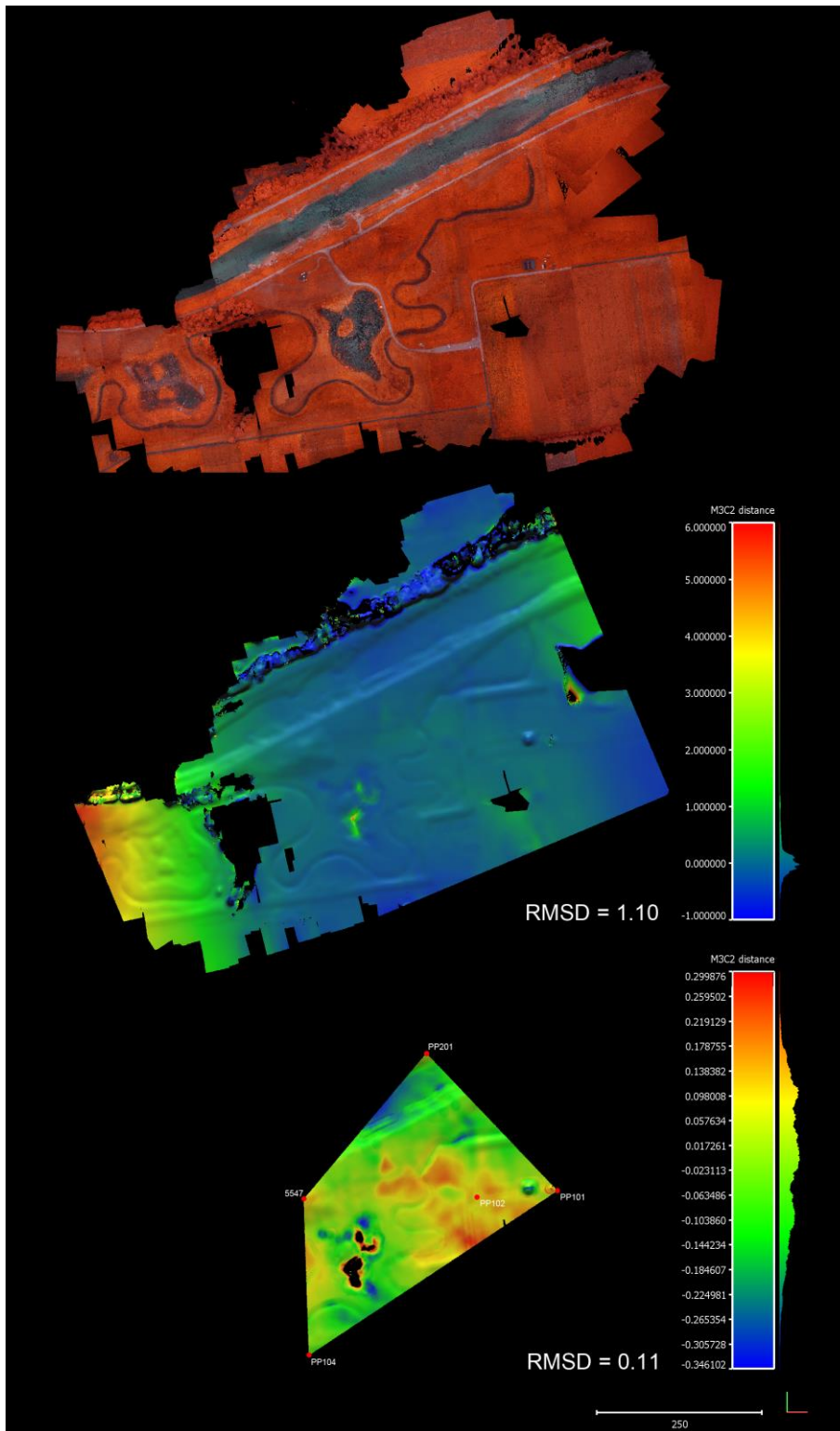


Fig. 29 A) Bramor mission 02.10.2015 NIR processed with GCP marker information included in the bundle adjustment B) M3C2 comparison of point cloud processed with GCP information included in the PhotoScan workflow and the same scene referenced in post processing using a seven parameter Helmert transformation. The cloud with GCP information is hereby defined as reference. Outside of the identified ground targets the alignment of two clouds worsens resulting in an overall RMSE of 1.10. C) Within the convex hull of GCPs used for referencing the cloud in post processing the RMSE is 0.11.